Emerging Technologies in Breast Imaging

Mary S. Newell and Anna I. Holbrook

Introduction

Mammographic screening has been validated as an effective way to decrease breast cancer deaths, responsible for a 30–40 % mortality reduction in participating populations. However, despite its success, it remains an imperfect tool, especially in certain subsegments of patients. Some cohorts for which mammographic evaluation proves less sensitive include women with dense breasts, women with genetic predisposition to breast cancers, and women with prior history of breast cancer. As a result, there is impetus to develop and refine new screening and diagnostic technologies that address the limitations of mammography. These include advanced mammographic applications such as digital tomosynthesis, stereoscopic mammography and contrast-enhanced digital mammography; dedicated breast computed tomography (CT); advanced applications of breast ultrasound and MRI; dedicated breast molecular imaging; and optical imaging. We describe these evolving technologies and outline their strengths and weaknesses.
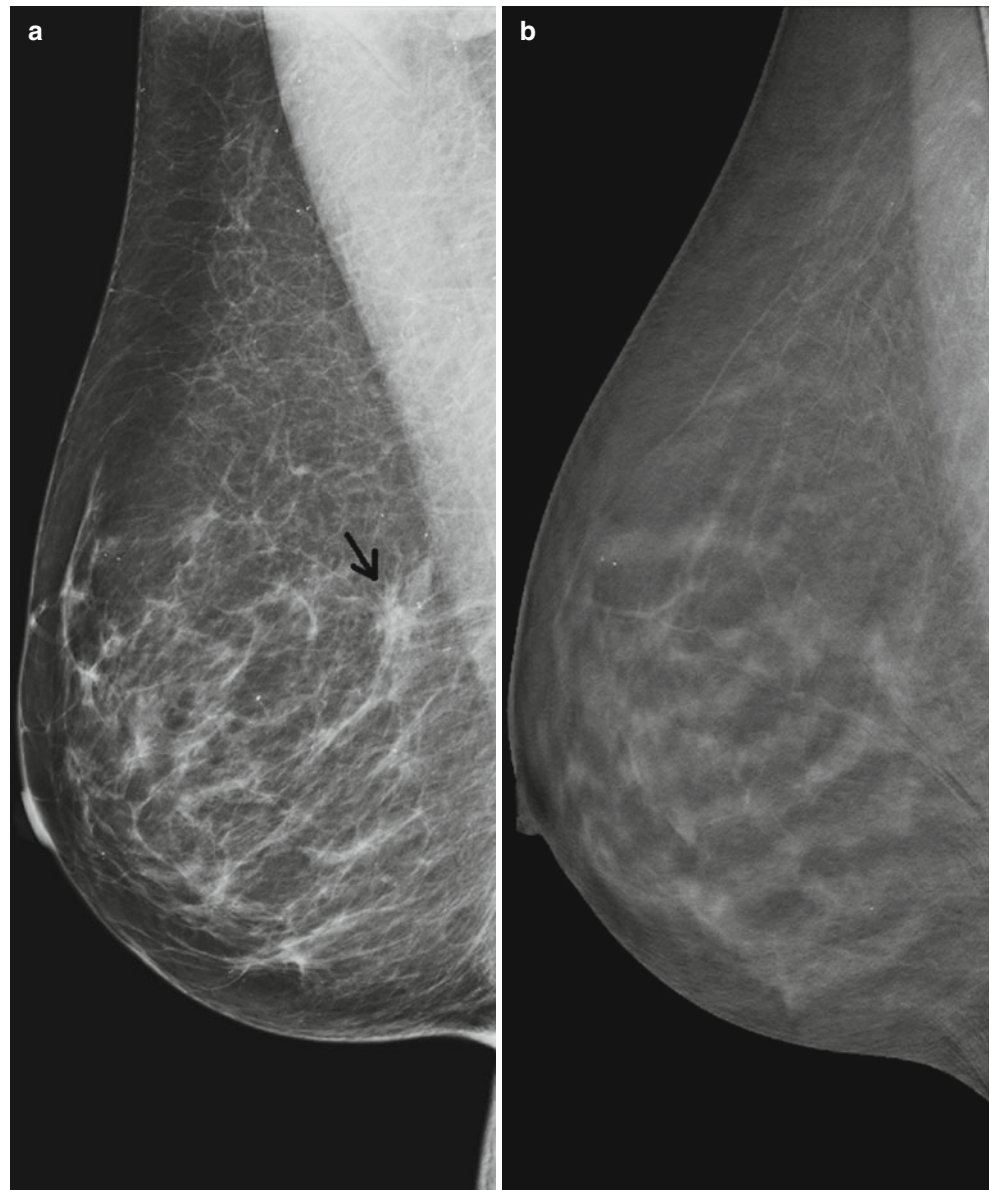
Tomosynthesis

Tomosynthesis is thought to improve detection of cancers and reduce false-positive exams by eliminating the overlap of normal fibroglandular tissue (Fig. 19.1a, b). In tomosynthesis, an x-ray tube is moved in an arc above the breast and detector, and multiple images are obtained as the tube moves. These images are then reconstructed, creating a series of individual in-plane images through the entire breast [1]. Tomosynthesis has showed promising results and in 2011 was approved by the FDA [2]. Waldherr et al. found

that one-view tomosynthesis had better sensitivity and negative predictive value than did full-field digital mammography (FFDM). This was true not only in dense breasts but also in fatty breasts. While 23 % of FFDMs required additional imaging to further evaluate a suspected abnormality, only 11 % of tomosynthesis exams did so [3]. Svahn et al. also found an improved sensitivity of one-view tomosynthesis when compared to FFDM (90 % vs. 79 %), but with no difference in false-positive exams [4]. However, data are conflicting when tomosynthesis is compared to FFDM, as some studies showed no difference in the diagnostic performance [5, 6].

In contrast, many studies have found optimistic results when examining tomosynthesis in combination with FFDM. Skaane et al. found that tomosynthesis in combination with mammography versus mammography alone resulted in a 27 % increase in the cancer detection rate ($p = 0.001$), with a 15 % decrease in false positives ($p < 0.001$). Also encouraging is that they found that adding tomosynthesis allowed for a 40 % increase in detection of invasive cancers [7]. Rafferty et al. had similar results, with a significantly increased area under the receiver operation characteristic (ROC) curve when tomosynthesis was combined with mammography compared to mammography alone. Recall rates for non-cancer cases significantly decreased for all readers. They also found that the increased sensitivity was greatest for invasive cancers [8]. Poplack and colleagues found a reduction of 40 % in the screening recall rate when tomosynthesis was used in addition to mammography [9], while Gur et al. found a decrease of 30 % [10]. A recent study by Rose and associates [11] found that after addition of tomosynthesis to FFDM in routine clinical practice, recall rates decreased from 8.7 to 5.5 % ($p < 0.001$), and the positive predictive value for recalls increased from 4.7 to 10.1 % ($p < 0.001$). Several studies have evaluated the use of tomosynthesis in lieu of additional mammographic views in characterizing noncalcified lesions. Some have found the two techniques to be comparable [12, 13], while Zuley et al. found that the area under the ROC curve (AUC) was significantly greater for

M.S. Newell, MD (✉) • A.I. Holbrook, MD
Department of Radiology and Imaging Sciences,
Emory University, Atlanta, GA 30345, USA
e-mail: mary.newell@emoryhealthcare.org;
anna.holbrook@emoryhealthcare.org

Fig. 19.1 (**a**) Mammogram
(MLO view) demonstrates an
area of possible architectural
distortion (*arrow*).
(**b**) Corresponding image from
tomosynthesis examination
shows no suspicious
abnormality. The distortion was
due to overlap of normal
fibroglandular tissue
(Images courtesy of Hologic®
and Carl J. D'Orsi, MD)

tomosynthesis versus supplemental mammographic views
(0.87 vs. 0.83) [14].

In order to decrease radiation dose and interpretation
time, single-view as opposed to two-view tomosynthesis
imaging has been explored. Wallis et al. found single-view
tomosynthesis examinations to have equivalent diagnostic
accuracy to a standard FFDM exam, while two-view tomo-
synthesis offered an improved accuracy, but only for readers
with less than 10 years of experience [15].

Tomosynthesis is thought to be less sensitive than mam-
mography for the detection of calcifications. This is due to
images being reviewed as slabs of user-defined thickness.
There is an inherent trade-off with the thickness of slabs:
thicker slabs allow for the perception of 3D clusters of

calcifications, but also lead to decreased spatial resolution of
each individual calcification [16]. Poplack et al. found that in
general, the image quality of calcifications was better with
mammography than with tomosynthesis [9]. However,
another study found that though FFDM was slightly more
sensitive than tomosynthesis for the detection of calcifica-
tions, the diagnostic performance as measured by AUR
between the two modalities was not significantly different
[16]. Further improvements in image acquisition and display
may lead to improvement in calcification detection. An addi-
tional drawback of tomosynthesis is an approximate dou-
bling of interpretation time when compared to mammography
alone [7, 15]. However, it is anticipated that this will be
balanced by reduction in recalled screening examinations,

follow-up studies, and biopsies [14]. Another limitation is increased radiation dose. Using tomosynthesis in combination with FFDM results in a doubling of radiation dose, though in many cases, this is still less than the FDA limit for a single standard mammogram exam [1, 8]. However, it is desirable to keep radiation doses as low as reasonably achievable. One solution to this is in the use of synthetically reconstructed two-dimensional images, created from the tomosynthesis data, in lieu of the additional corresponding full-field view. This technology has recently been approved by the FDA [17].

Stereoscopic Mammography

Similar to the idea behind tomosynthesis is that of stereoscopic mammography, which attempts to overcome 2D mammography's limitation of overlying normal tissue obscuring and mimicking lesions. Stereoscopic imaging uses two images of the breast acquired above and below the 0° axis. These images are viewed with cross-polarized glasses on a display consisting of two cross-polarized monitors at 110° from one another, each displaying one of the images, and a silver-coated glass plate bisecting the 110° angle (Fig. 19.2). In this setup, each eye sees only one of the two images, and the reader's visual system fuses the images into a single in-depth image. One study that evaluated stereoscopy clinically found that it had significantly higher specificity and accuracy and a lower recall rate when compared to standard mammography, with a similar sensitivity [18]. Further research will need to be done to confirm these results and to see if good results can be obtained at a lower radiation dose.
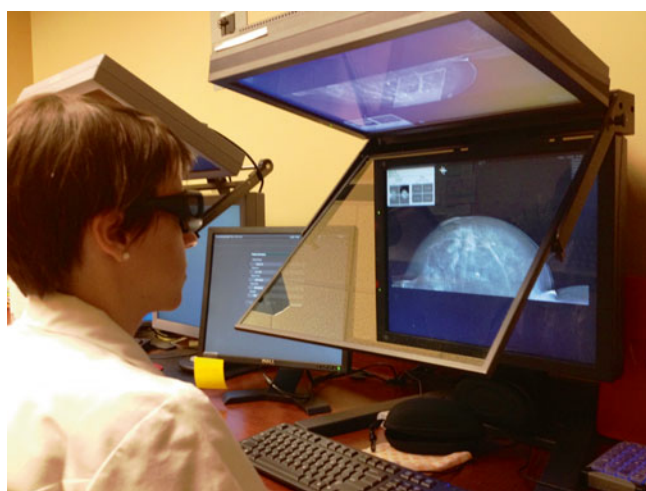

Fig. 19.2 Stereoscopic mammographic dedicated viewing station
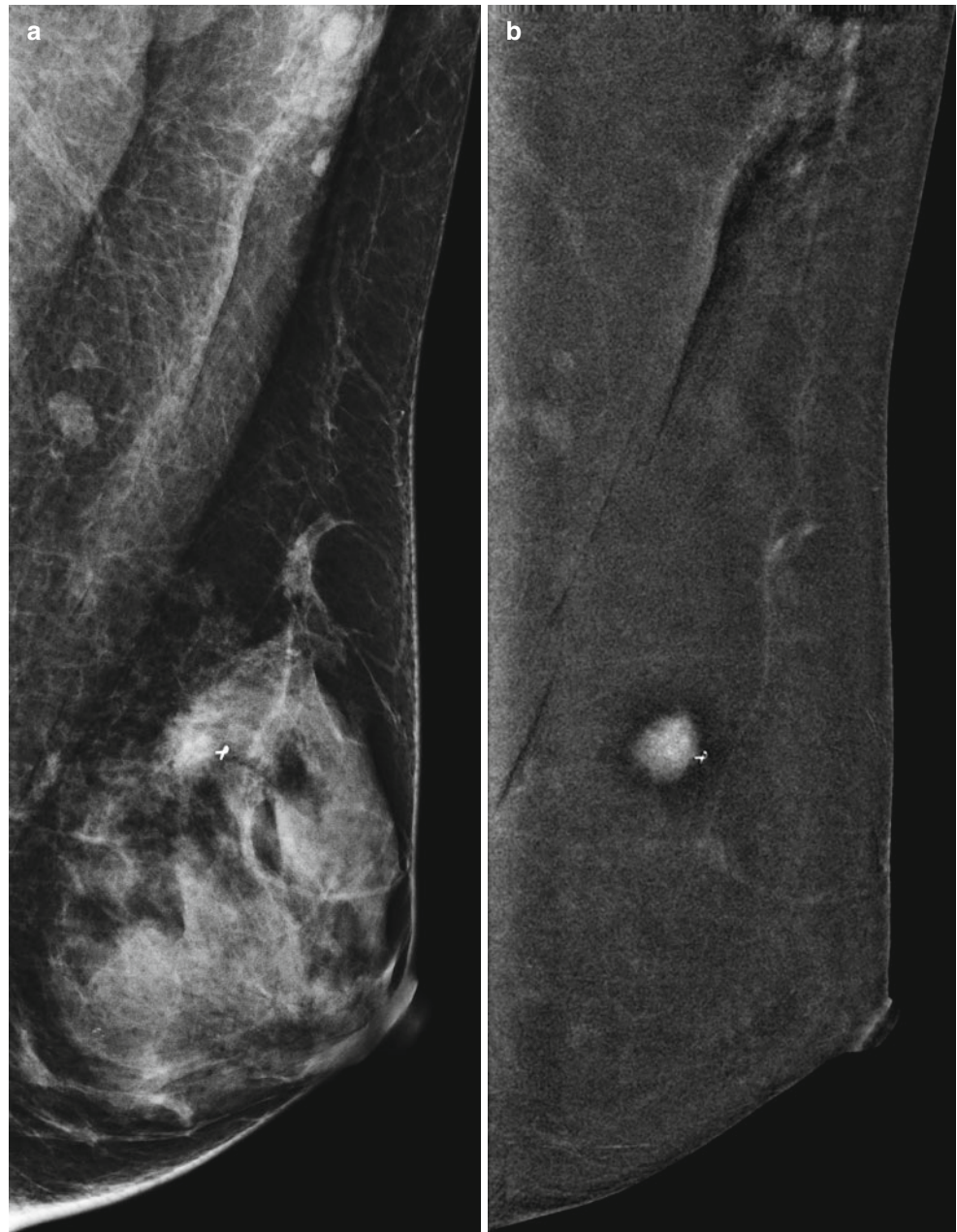
Contrast-Enhanced Mammography (CEM)

Another modification that has been developed to overcome the limitations of conventional mammography is the addition of intravenous contrast. This is postulated to improve lesion detection due to the preferential uptake of contrast material within cancers, as seen in contrast-enhanced MRI (magnetic resonance imaging). Contrast-enhanced mammography could theoretically be an alternative for those unable to have an MRI.

There are two methods of obtaining contrast-enhanced mammographic images. One is to use temporal subtraction, in which a pre-contrast mask image is obtained followed by the injection of contrast and a series of additional exposures [19]. The mask image is then subtracted from those taken after contrast injection to show the distribution of contrast. This method is limited by the requirement for compression, motion artifacts due to long imaging times, and the ability to only image one breast in one view per injection. Another method uses dual-energy acquisition, in which, after iodinated contrast injection, two images are performed in rapid succession—a low-energy image below the k edge of iodine (33.2 keV) and a high-energy image above the k edge. The high-energy image preferentially demonstrates the contrast distribution, as photons just above the k edge are more likely to be attenuated by iodine than those below or far above it [20]. The images are then processed to suppress background breast tissue and highlight iodine-enhanced areas [21] (Fig. 19.3a, b). This dual-energy technique allows both breasts to be imaged in multiple views with only one injection [22]. It also permits shorter acquisition times, minimizing motion artifact and the duration of breast compression [22]. A disadvantage of this method is that as contrast is present on both acquisitions, some of the iodine is subtracted out of the processed image [20].

An initial study by Jong et al. showed that with the temporal subtraction method, 8/10 (80 %) cancers enhanced and 7/12 (58 %) benign lesions did not [23]. Another preliminary investigation by Diekmann and associates found that by using temporal subtraction, contrast could be seen within known tumors in all seven participating patients [24]. A subsequent study showed that adding temporal subtraction CEM to conventional mammography increased sensitivity for detecting cancer from 43 to 62 %. The improvement in sensitivity was even greater in patients with dense breasts [25]. Another study of temporal subtraction CEM found that its sensitivity for known cancers was 80 % [26]. Interestingly, in 2 of 20 patients, the cancers were in the posterior part of the breast and moved out of the field of view between the mask and contrast-enhanced images. This highlights one of the limitations of the temporal subtraction technique: prolonged acquisition times resulting in patient motion.

Fig. 19.3 A 48-year-old with grade 1 invasive ductal carcinoma, post biopsy. (**a**) Standard MLO view mammogram. (**b**) Dual-energy contrast-enhanced digital mammogram (CEDM). The cancer is not readily apparent on standard mammography (**a**) but is well demonstrated on CEDM (**b**) (Images courtesy of John Lewin, MD)

A preliminary study of the feasibility of duel-energy contrast-enhanced (DE CE) mammography was done by Lewin et al. [27]. They demonstrated that all 14/14 cases of cancer enhanced, while out of 12 patients with benign lesion, only 4 enhanced. Jochelson and associates compared DE CE mammography with conventional mammography and with MRI in 52 patients with known cancer [21]. They found that DE CE mammography and MRI both had a sensitivity of 96 % for index tumors, more than conventional mammography, which had a sensitivity of 81 %. Sixteen of the 52 patients had multifocal or multicentric cancers, and MRI was better at detecting these additional ipsilateral cancers than

was DE CE mammography (88 % vs. 56 %). However, MRI had more false-positive findings (13/52 or 25 %) than did DE CE mammography (2/52 or 4 %). The Jochelson study found that the size of lesions as measured on DE CE mammography accurately represented the pathologic size in all but two patients, in which it overestimated the size by 1 and 1.7 cm. MRI accurately depicted the size in both. Another study, however, found that there was a good correlation between the size of lesions as measured on CE mammography and histological specimens (coefficient of correlation of 95 %) [26]. Dromain et al. [19, 22] found that diagnostic accuracy was improved when DE CE mammography was performed

in addition to conventional mammography with or without ultrasound when compared to conventional mammography with or without ultrasound alone. The area under the ROC curve increased for each reader when DE CE mammography was added to conventional mammography +/− ultrasound.

Interestingly, unlike the rapid washout of contrast seen in malignancies during MRI imaging, enhancement with CE mammography remains present for at least 10 min. This may be due to differences between gadolinium and iodine [21] or as a consequence of breast compression [26]. Because of this lack of washout, kinetic enhancement information is not a helpful discriminator in CE mammography as it is in MRI [25].

Limitations of contrast-enhanced mammography include a decreased ability to evaluate the breast periphery due to a rind of increased density from radiation scatter [19, 21]. Additionally, there is a small increase in radiation exposure compared to conventional mammography. Several authors have calculated that the total additional radiation dose was equivalent to approximately one additional mammographic view [21, 22]. Lastly, there is a possibility of allergic reaction to the iodinated contrast, which can be life-threatening [22]. More studies will need to be done to verify that the risks are justified by a significant improvement in the detection of cancer.

Breast Ultrasound

Background

The appeal of using breast ultrasound (US) as a diagnostic adjunct to mammography was first noted in the 1960s–1970s, related to its "nondestructive technique" [28]. Kobayashi and colleagues reported early success using ultrasound to differentiate between benign and malignant breast lesions, employing a 5 MHz transducer and an automated system. They reported 84 % accuracy in predicting benign pathology and 90 % accuracy with malignant lesions, using only two sonographic criteria, which roughly correlate in today's terminology to (1) the echo pattern of the lesion itself and surrounding tissue (the latter actually concentrating on the posterior lesion margin) and (2) lesion posterior acoustic features [29]. Their cohort consisted only of palpable lesions that were suspicious enough to warrant excision/mastectomy, however. In addition, the smallest mass they were able to find was 5 mm, even when they were directed to the site in question by clinical findings. Dodd and associates concluded that US lacked the spatial resolution to detect and characterize subclinical cancers [28]. As a result, breast US was largely relegated to differentiating cystic from solid masses detected clinically or mammographically, at which it proved skillful. As sonographic equipment became more sophisticated, with resolution improved by the introduction of higher-frequency transducers of at least 10 MHz, US became
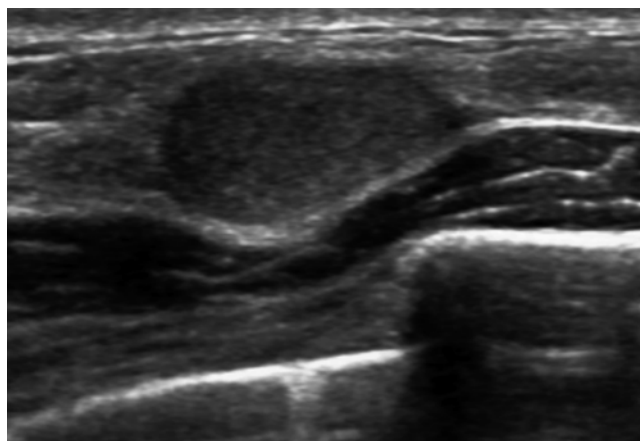

Fig. 19.4 This mass shows multiple features (gently lobulated margins, oval shape, parallel orientation, homogeneously mild hypoechogenicity, absence of suspicious features) that allow surveillance rather than biopsy, despite its solid nature

an increasingly sought-after tool to supplement mammography in the evaluation of breast problems. Multiple studies have confirmed its utility in determining which mammographically detected solid masses might undergo short-term surveillance rather than requiring biopsy (negative predictive value in the region of 99.5 %), assuming strict morphologic criteria were followed [30, 31] (Fig. 19.4).

As the ability of breast US to find and characterize mammographically occult lesions became validated, the possibility of using US as an adjunct screening tool, at least for women at increased risk and/or with dense tissue, has gained momentum. ACRIN (American College of Radiology Investigational Network) 6666, a prospective multicenter study, was designed to compare mammography alone to mammography plus ultrasound in a screening setting, using a cohort of patients at elevated risk for breast cancer and heterogeneously or extremely dense breast tissue in at least one quadrant as determined by mammogram. Among their 2,637 patients, 12 cancers were seen on ultrasound alone, representing a supplemental yield of 4.2 cancers per 1,000 over mammography alone. The cancers found with US alone tended to be smaller and more often node negative [32]. Two additional multicenter studies have confirmed the results noted in ACRIN 6666 [33, 34], showing additional cancer detection yield of 4.2–4.4 per 1,000.

However, breast US has limitations, including imperfect specificity and, at least in the screening setting, many false positives. ACRIN 6666 revealed a near doubling of false-positive rate (8.1 % vs. 4.4 %), a lower positive predictive value for biopsy (PPV_2) (8.9 % vs. 22.6 %), and a higher rate of short-term follow-up recommendation (8.6 % vs. 2.2 %) with US alone compared to mammography. Thus, the additionally detected cancers came with a "price," including unnecessary biopsies and added work-up. Another limitation includes its
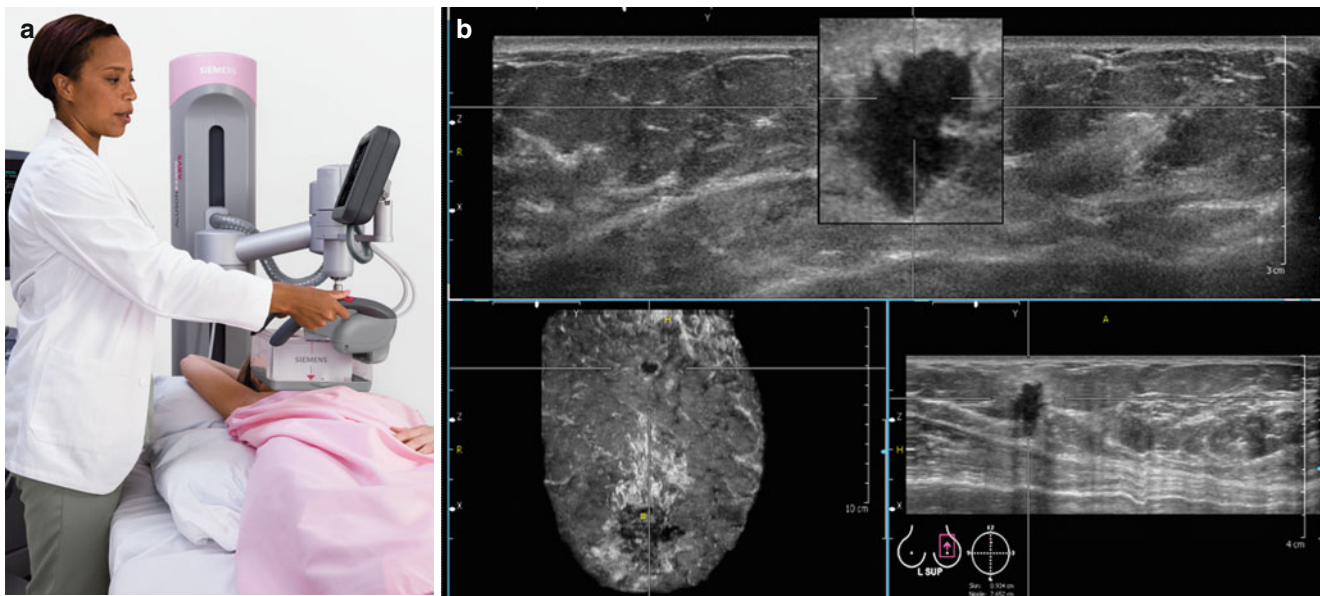
Fig. 19.5 (**a**) Automated whole-breast ultrasound unit with large footprint transducer covering breast. (**b**) Breast cancer outlined in three orthogonal views (Images courtesy of Siemens Healthcare)

diminished sensitivity for in situ cancers compared to mammography [32]. Handheld technique is also highly operator dependent: given its real-time nature, if a lesion is not detected and recorded during active scanning, it will be missed. In a screening setting, it is time and labor intensive, especially of concern when requiring physician scanning involvement during times of decreasing technical and professional reimbursement. In ACRIN 6666, the reported average scan time per patient was 19 min for a bilateral exam (often much longer in patient with large breasts or multiple findings), excluding time spent talking to the patient, reviewing and reporting the exam, and comparing to prior exams [32]. Evolving ultrasound technology is primed to address many of these limitations.

New Technologies

Automated whole-breast ultrasound (AWBU) is being revisited, improved, and refined after its introduction in the 1960s–1970s. AWBU has the potential to standardize and expedite study acquisition. It theoretically can be performed by a technologist without requiring physician involvement during scanning. A variety of prototypes are under development and clinical evaluation. Each uses unique acquisition and presentation methods and employs high-frequency probes. One vendor uses a robotically guided but standard transducer to scan the entirety of both breasts, with presentation of the images in a cine loop in 2D axial projection. Another employs a large footprint transducer placed over the central part of each breast with patient supine, with presentation of the reconstructed images in the coronal plane, as well as the orthogonal source images (Fig. 19.5a, b). A third prototype makes use of a custom transducer to scan a pendant, immersed breast, with

presentation of 3D reconstructed images [35]. Wang and colleagues showed that the diagnostic accuracy of AWBU in differentiating benign from malignant lesions is comparable to handheld US [36]. A 2010 multicenter prospective screening study comparing mammography to automated whole-breast screening showed that automated US screening resulted in an increase in cancer yield by 3.6 per 1,000 compared to mammography alone [37]. These authors also found an improved PPV (30.7 % vs. 8.9 %) and a higher detection rate of subcentimeter US-only cancers (14.3 % vs. 6.2 %) when their automated technique was compared to the handheld technique used in ACRIN 6666. These results require validation by other large studies, but suggest the potential efficacy of AWBU for increasing throughput in a screening setting, while retaining accuracy. Some potential limitations of AWBU included its limited field of evaluation (the axillae and, with some systems, the periphery of the breasts are excluded) and diminished effectiveness with large breasts (deep lesions may not be well visualized/characterized). As specialized add-on equipment or complete replacement systems will be required to carry out AWBU, cost will rise.

Ultrasound elastography (USE) is another exciting emerging technology that may improve specificity for lesions detected with ultrasound, aiding in more cost-effective but equally safe management of these lesions. USE essentially evaluates the stiffness of tissue, as is done more grossly and subjectively during physical examination of the breast. Two types of USE are currently being evaluated: compressive (strain) elastography and shear-wave elastography (SWE). In each, one can ascertain the stiffness of a mass and its adjacent environment by observing its reaction to the application of an external stressor. With compressive elastography, gentle transducer pressure is used to apply external force (stress) to the surface of the breast over the
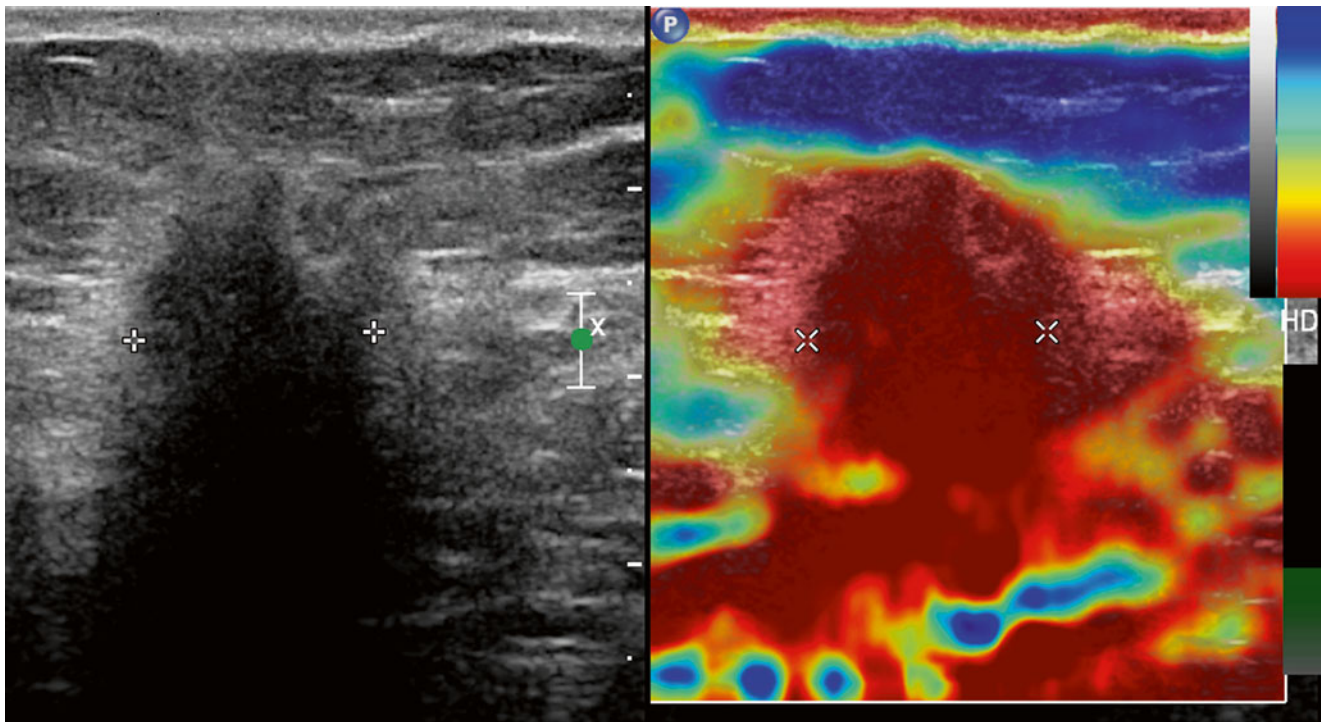
Fig. 19.6 Compression elastography. A mass is seen on standard US image (*left*). The corresponding elastogram (*right*) shows the mass to display low strain (assigned *red* here), indicating a firm consistency compared to other breast tissue. Note that the red coloration extends beyond the margins of the mass as outlined by cursor placement, indicating an Itoh score of 5

lesion in question; the resultant "strain" (the degree to which the tissue changes in shape, size, and position when the stress is applied) has implications about likelihood of malignancy. Upon detection of an equivocal lesion during real-time scanning, elastography software allows side-by-side display of the B-mode image and the corresponding "elastogram" (a color-coded visual display of the semiquantitative strain data generated automatically and behind the scenes) (Fig. 19.6). This elastogram is then qualitatively evaluated and/or assigned a score, as described by Itoh and associates [38]. They described a spectrum of elastogram patterns: a lesion displaying uniform high strain (diffusely soft and malleable) would receive a score of 1; at the other extreme, a lesion and its surrounding tissue showing low strain (firm and immobile) would receive a score of 5. A meta-analytic comparison of USE to conventional B-mode (*N*=5,511 lesions) showed an improvement in specificity from 70 % (B-mode) to 88 % (USE) [39]. However, USE alone was far less sensitive than conventional US (79 % vs. 96 % for B-mode), demonstrating that this technique cannot serve as a replacement for conventional US, but rather as a triage tool that may allow safe deferral of biopsy of borderline suspicious (i.e., BIRADS (Breast Imaging and Reporting System) 4a) lesions which have a low elastography score, thereby decreasing the unacceptably high false-positive rate of screening US. This method of USE has some intrinsic limitations. It is operator dependent (related to subjective application of "light" transducer pressure as the source of mechanical stress) and semiquantitative in nature and therefore may lack reproducibility [40].

Shear-wave elastography (SWE) represents another method of interrogating the stiffness of tissue. Instead of relying on transducer pressure to stress tissue, SWE measures tissue stiffness by calculating the speed at which that tissue variably propagates shear waves. These shear waves are generated as a result of a transducer-produced acoustic radiation force impulse (ARFI), which perturbs the tissue (Fig. 19.7). Ultrafast scanning is required to record the minute degrees of tissue displacement that occurs as the transversely oriented shear waves travel through tissue at varying speeds, depending on tissue stiffness. As the stress imparted by this pulse wave is known, the resultant strain of the interrogated tissue can be quantified. SWE requires no active participation by the technologist over and above scanning and therefore is operator independent and highly reproducible. Therefore, SWE mitigates many of the limitations of strain elastography. This technology is coupled with B-mode imaging. Research is ongoing to determine which single or combination of elastographic features (e.g., quantitative features such as maximum, median, or minimum elasticity value; elastographic lesion homogeneity; elastographic shape; elastographic lesion size vs. B-mode size) serve best to improve specificity and even sensitivity. Results of the BE1 Multinational Study [41] comparing conventional US to US plus SWE confirmed that by considering certain elastographic features, some BIRADS 4a lesions could be safely downgraded. In addition, some BIRADS 3 (and even BIRADS 2) lesions were accurately upgraded: 4 of 4 BIRADS 3 lesions that were morphologically benign appearing but showed suspicious elastographic
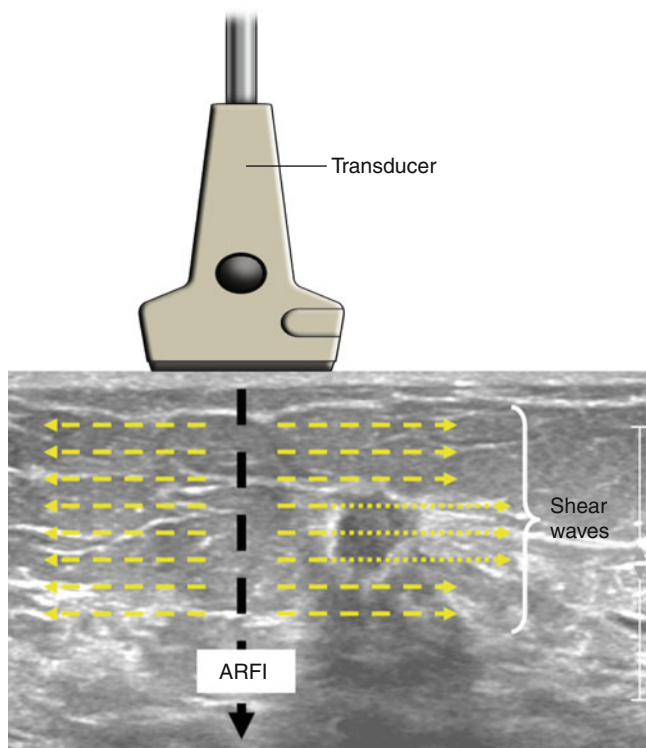
Fig. 19.7 Schematic of shear-wave propagation. An acoustic wave force impulse (*ARFI*) is sent from transducer into breast, resulting in propagation of transverse shear waves. These waves traverse the mass present here faster than normal tissue and can be quantified and visually displayed

Fig. 19.8 Dedicated breast CT scanner. The patient lies prone and hangs breast in vertical gantry (*arrow*) (Courtesy of Ioannis Sechopoulos, PhD)
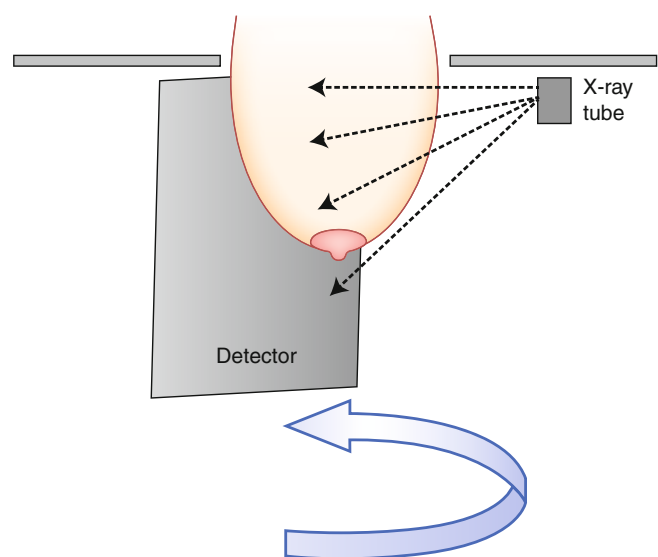

Fig. 19.9 Schematic of dedicated breast CT scanner. The X-ray source consists of a half cone beam (collimated to target only breast) and detector, both of which rotate in synchronized opposition around the pendant breast

features proved to be cancer. By adding SWE, specificity was increased from 61.1 to 78.5 %. Both SWE and strain elastography allow accurate differentiation of complicated cysts from solid masses, a situation encountered frequently when using US in both the screening and diagnostic arenas, allowing improvement in specificity and diminishment in false-positive biopsy and short-term follow-up rates.

The use of computer-assisted diagnosis (CADx) for US is another way that improved performance can likely be realized. As opposed to computer-assisted detection technology used in mammography, US CADx is used not to detect lesions but to help predict their likelihood of malignancy once detected, based on combined morphologic features. Kashikura and associates showed that reader accuracy (as measured by AUC) on the average improved from 0.716 to 0.864 ($p = .006$) when CADx was used by three experienced imagers to help evaluate a series of 390 US masses [42].

Dedicated Breast Computed Tomography

Dedicated breast computed tomography (DBCT) represents an additional investigational modality that seeks to address the 2D limitations imposed by standard mammography. Its

theoretical appeal includes the ability to image and display the breast in isotropic three-dimensionality, as has been exquisitely demonstrated when imaging other organs, and the lack of need for breast compression.

Several prototype models are undergoing evaluation. They are configured such that the patient lies prone on a table with her breast placed pendant into a dedicated gantry (Fig. 19.8). Rather than traditional cone beam geometry used for whole-body CT, a half cone beam is used, dictated by the need for the X-ray tube and the detector to rotate as closely opposed to the undersurface of the table as possible to allow visualization of posterior breast tissue and, optimally, a portion of chest wall (Fig. 19.9). Flat panel detectors are used, with a 40×30 cm field of view (PAXSCAN™ detector, Varian Imaging Systems®, Salt Lake City, UT, USA). A variety
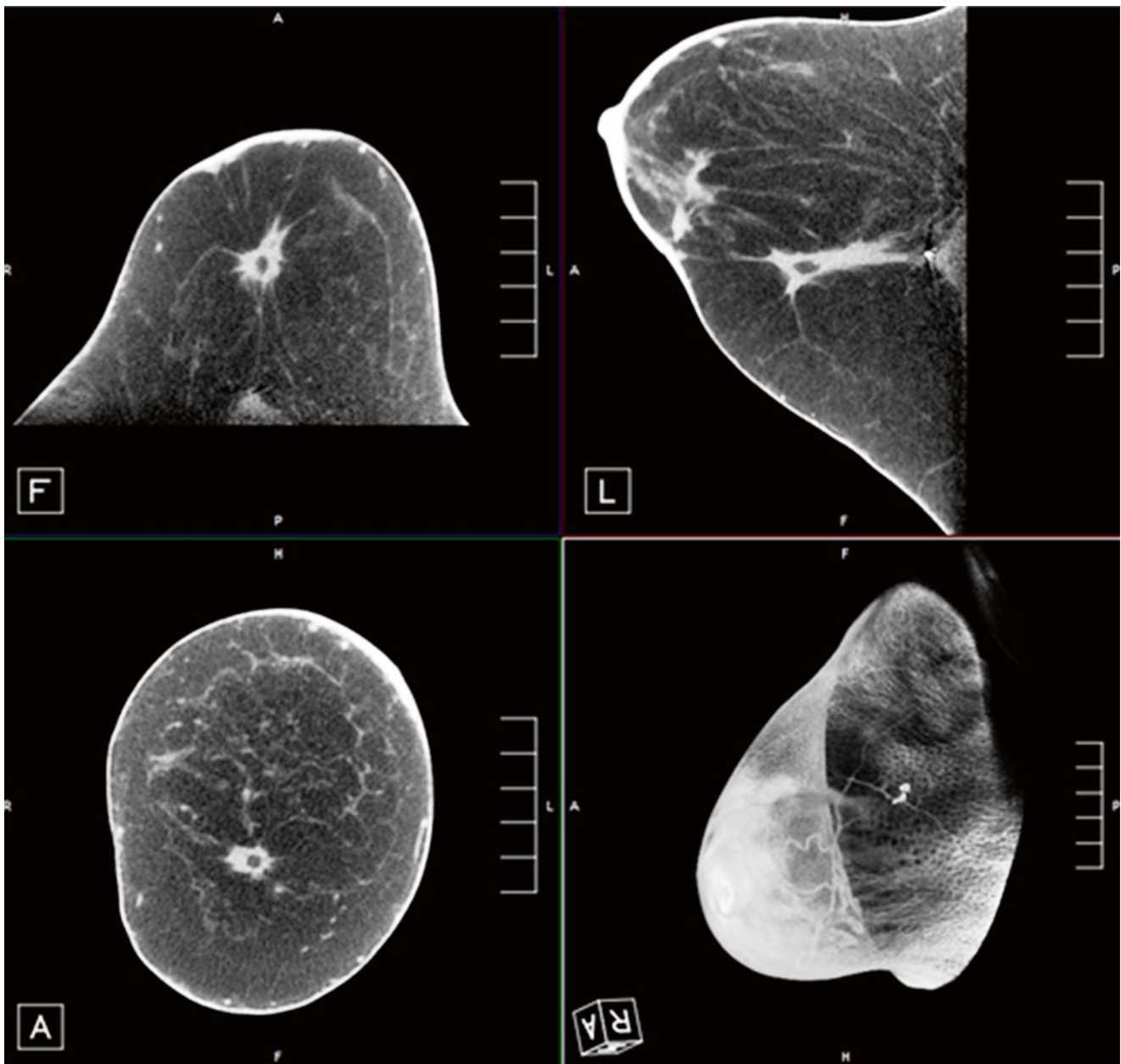
Fig. 19.10 Non-contrast breast CT. A mass (showing spiculated margins but central fat: fat necrosis) is displayed in three orthogonal views. A maximum intensity projection (*lower right*) is also displayed, which can be rotated in any projection (Courtesy of Hologic® and Carl J. D'Orsi, MD)

of X-ray source types has been employed, operating at kVps from 49 to 80, with resultant scan times ranging from 10 to 16.6 s, allowing single breath hold [43]. These original prototypes allow spatial resolution in the range of 150–400 μm, less than is achieved with standard digital mammography [44]. The images are reconstructed in three orthogonal planes and evaluated by scrolling through an imaging volume. 3D and maximum intensity projection (MIP) can be created as well (Fig. 19.10). Using this general technique, radiation dose per breast per series is comparable to a two-view mammogram [45].

Adequacy of breast coverage was evaluated by O'Connell and associates. They found that greater tissue inclusion was demonstrated medially, laterally, inferiorly, and posteriorly, with equivalent coverage noted superiorly. However, by using axillary nodes as a marker for comparison, they noted that mammography allowed better coverage of axillary tail. Patient acceptance must be considered in evaluating this modality, since avoidance of breast compression is touted as a potential advantage. O'Connell's group also assessed patient acceptance and comfort. A minority of patients (13 %) found DBCT to be less comfortable than mammography, with most

finding it more (43.5 %) or equally (43.5 %) comfortable compared to mammography [45].

The clinical data regarding DBCT are relatively sparse. Initially, work was done without the use of intravenous contrast. Lindfors and colleagues scanned a cohort of 69 women with BIRADS 4 or 5 lesions, as well as 10 healthy volunteers. They compared DBCT images to the patients' mammograms in a nonblinded fashion for lesion conspicuity. Overall, there was no difference in lesion detectability between modalities; however, masses were better seen with DBCT, and calcifications were better detected with mammography, reaching significance in both scenarios [46]. These data were confirmed on follow-up studies by the same group [43] and suggest that the lack of comparable spatial resolution achieved with the original DBCT prototypes limits the clinical efficacy of DBCT, at least in the non-contrast setting, when evaluating calcifications. O'Connell et al., using a different prototype scanner, also found, in comparing mammography to non-contrast DBCT, that CT was inferior in detecting calcifications when compared to mammography. In their study, 13.5 % of calcifications seen on mammography were not detectable on DBCT [45].

Non-contrast DBCT is dependent on morphology and differences in intrinsic soft tissue contrast to allow lesion detection. More recent work has looked at leveraging the physiological differences between normal parenchyma, benign tumors, and malignant lesions by using intravenous contrast material, as has been done with breast MRI. In a study of similar design to that described previously, Prionas and associates compared mammography and non-contrast DBCT to contrast-enhanced DBCT (CE-DBCT) in 46 women with BIRADS 4 or 5 lesion who underwent all three imaging studies prior to biopsy. They found that all malignant lesions ($N=29$) were better seen on CE-DBCT than on mammography, especially masses. Interestingly, malignant calcifications ($N=7$; 5 of 7 were pure DCIS) were also better seen on CE-DBCT, albeit only slightly and not reaching statistical significance. Conversely, benign calcification was seen with greater conspicuity on mammography, raising the possibility that CE-DBCT might allow for greater specificity in calcium evaluation by essentially "missing" benign calcifications. Since degree of enhancement is quantifiable, these investigators were able to show that differential enhancement may allow prediction of malignancy, with an area under the ROC curve of 0.876 [47].

The logistics of CE-DBCT deserve consideration. One of the benefits of dynamic contrast-enhanced (DCE) MRI is that robust temporal and spatial information is obtained with technology that allows parallel imaging of both breasts synchronously. With DBCT, however, only one breast is imaged at a time. It has not been established how best to combine the imaging of both breasts with the timing of contrast administration. Prionas' group [47] used the following scan sequence:

pre-contrast unaffected breast, pre-contrast affected breast, post-contrast affected breast, and post-contrast unaffected breast. Therefore, two patient position changes were required. Obviously, some kinetic data are lost in this situation when compared to DCE MRI, where multiple sequential and bilaterally parallel postcontrast time points are acquired. This group, however, noted that morphology is likely more important than kinetics when evaluating lesions, and DBCT with its superior resolution, may make this logistical point relatively moot. Further study is needed to validate that observation. Prionas' group also reported that decisions regarding contrast dose and delay after injection were derived empirically. Again, ongoing work will help determine optimal scanning protocols.

The early work regarding DBCT appears promising. In an interesting discussion of what the "perfect" replacement for mammography would look like, Kalender et al. noted that that tool must meet the following specifications: 3D capabilities, good soft tissue contrast, dynamic/kinetic proficiency, high spatial resolution (100 μm), dose comparable to two-view mammography, patient comfort without need for significant compression, biopsy capabilities, and low cost [48]. It appears from these studies that DBCT comes close to meeting this challenge. However, a few concerns remain. The original prototype models, on which the available clinical studies have been performed, offer spatial resolution in the range of 300–400 μm, inferior to that demanded by Kalender. However, several groups are working on new prototypes that achieve improved resolution while maintaining acceptable dose, using spiral technique and other modifications [48, 49]. Additionally, a "clinic-ready" fully shielded model has been developed that employs an open geometry which will allow integration of a (yet-to-be-developed) biopsy system. Its developers indicate that a clinical throughput of 11 min/patient can be expected and a cost comparable to a tomosynthesis unit [49]. Even the original prototypes achieve a rapid per-sequence scan time of 10–16 s. Thus, the kinetic considerations will likely be addressed. These new prototypes await clinical validation. Although it appears that the theoretically "perfect" breast imaging machine has nearly been built, it remains to be seen if DBCT can garner the excitement that DCE breast MRI and tomosynthesis have.

Magnetic Resonance Imaging

Magnetic resonance imaging (MRI) has been validated as a robust breast imaging tool, largely related to its high sensitivity for detection of breast cancer, in the range of 94–99 %. Its many indications include high-risk screening, determination of the extent of disease in newly diagnosed breast cancer patients, assessment of treatment response in

patients undergoing neoadjuvant hormonal or chemotherapy, problem-solving in selected cases where a suspected imaging finding can be neither dismissed safely nor validated/localized by standard imaging, and further evaluation of suspicious clinical symptoms where a biopsy target or cause cannot be identified by routine imaging. However, it suffers from some drawbacks, including reported relative low specificity (range 37–86 %) [50] and high cost, when compared to mammography. Newer technologies, which explore parameters other than lesion morphology and kinetic enhancement characteristics, are being developed to address these limitations.

Magnetic Resonance Spectroscopy (MRS)

Magnetic resonance spectroscopy interrogates the chemical composition of tissue in vivo in a noninvasive manner. This technique has been applied to the brain and prostate with success and continues to undergo investigation for use in breast cancer evaluation. The bulk of chemical material in the breast consists of water and fat. However, other molecules can be detected via MRS, including some relatively specific for breast neoplasia, namely, choline-containing compounds (grouped together and referred to as total choline). These molecules have a role in membrane synthesis and metabolism and therefore may serve as signature molecules for the presence of breast cancer, where such metabolism is elevated. This total choline is present in high enough concentrations that its presence can be detected by the small magnetic field alterations its protons create (Fig. 19.11a, b). Choline can be present in normal breast tissue and benign breast lesions, indicating that quantification and not just identification of its presence is paramount [51]. One appealing potential use for MRS would be to increase the specificity of MRI. Bartella and associates found that by incorporating MRS into the MR protocol, the positive predictive value of biopsy could be increased from 35 to 82 %, with MRS showing specificity of 88 %, while maintaining 100 % sensitivity [52]. Dorrius and colleagues showed that BIRADS 3 lesions could be accurately reassigned based on choline concentrations. In their study, the use of MRS would have allowed proper identification of the two of eight malignant lesions initially called BIRADS 3 on routine MRI as well six of eight benign lesions that could have been safely reassigned to the BIRADS 2 category. There was no overlap between the choline concentrations of benign and malignant lesions, and their AUC was 1.00, compared to 0.0964 for standard MRI [53]. However, both studies only interrogated lesions 1 cm or greater in size. Tozaki's results were less compelling, showing overall sensitivity and specificity of 44 and 85 %, respectively. When only lesions >1.5 cm were considered, sensitivity increased to 82 % but specificity fell to 69 % [50].

Another area where MRS may be useful is in the early prediction of treatment response to neoadjuvant chemotherapy (NAC). An optimal tool would allow prediction as early in treatment as possible, to allow midcourse regimen change in nonresponders. Mammography, ultrasound, and physical exam rely on decrease in tumor size as a marker of response, but this has been shown to be unreliable in some cases and may lag behind real response. MRI is a more accurate tool, as it can show physiologic changes that may precede size change [54]. However, as MRS is measuring tumor metabolites in the form of choline compounds, it could provide even more specific information about treatment response and cell death. Meisamy showed that using a 4 T unit, changes in tumor choline concentrations could be detected within 24 h after treatment initiation [55]. Tozaki used a 1.5 T unit to show that this indication was feasible with current clinically available hardware and found that tumor choline was reduced after two treatment cycles in eventual responders compared to nonresponders, despite no significant change in tumor size at that point between the two groups. Positive and negative predictive values were 89 and 100 %, respectively [56].

MRS is hampered by several limitations. Lesion size is one. Most studies have narrowed inclusion criteria to lesions ≥1 cm, as partial volume averaging makes specific detection of choline difficult in smaller lesions. This decreases its utility for lesion characterization/management, especially in non-mass enhancements. However, Razek and colleagues were able to show improved sensitivity and specificity over MRI for lesion characterization even for lesions as small as 0.5 cm with MRS, when using a 3 T system. They attribute their favorable results to higher field strength [57]. Other limitations of MRS include low sensitivity for detection of DCIS, as choline is often absent in in situ lesions; the capability of examining only a single lesion when single-voxel technique (most common) is used; and false-negative exams, especially when inadequate fat suppression allows the spectroscopic peak of fat to broaden and obscure the relatively small choline peak. Additionally, no commercial analytic software has been developed specific to breast MRS [58]. Therefore, for several reasons, MRS remains outside of routine clinical practice at this point, but holds promise.

Diffusion-Weighted Imaging (DWI)

Diffusion-weighted imaging is another emerging MRI technique that probes lesion physiology and local architecture rather than just morphology and kinetic characteristics. It assesses the ability of water to move freely and randomly in tissue (Brownian motion). This motion may be relatively restricted under certain circumstances, such as in the presence of increased cellular density, cellular swelling, changes in membrane permeability, and the presence of cell lysis.
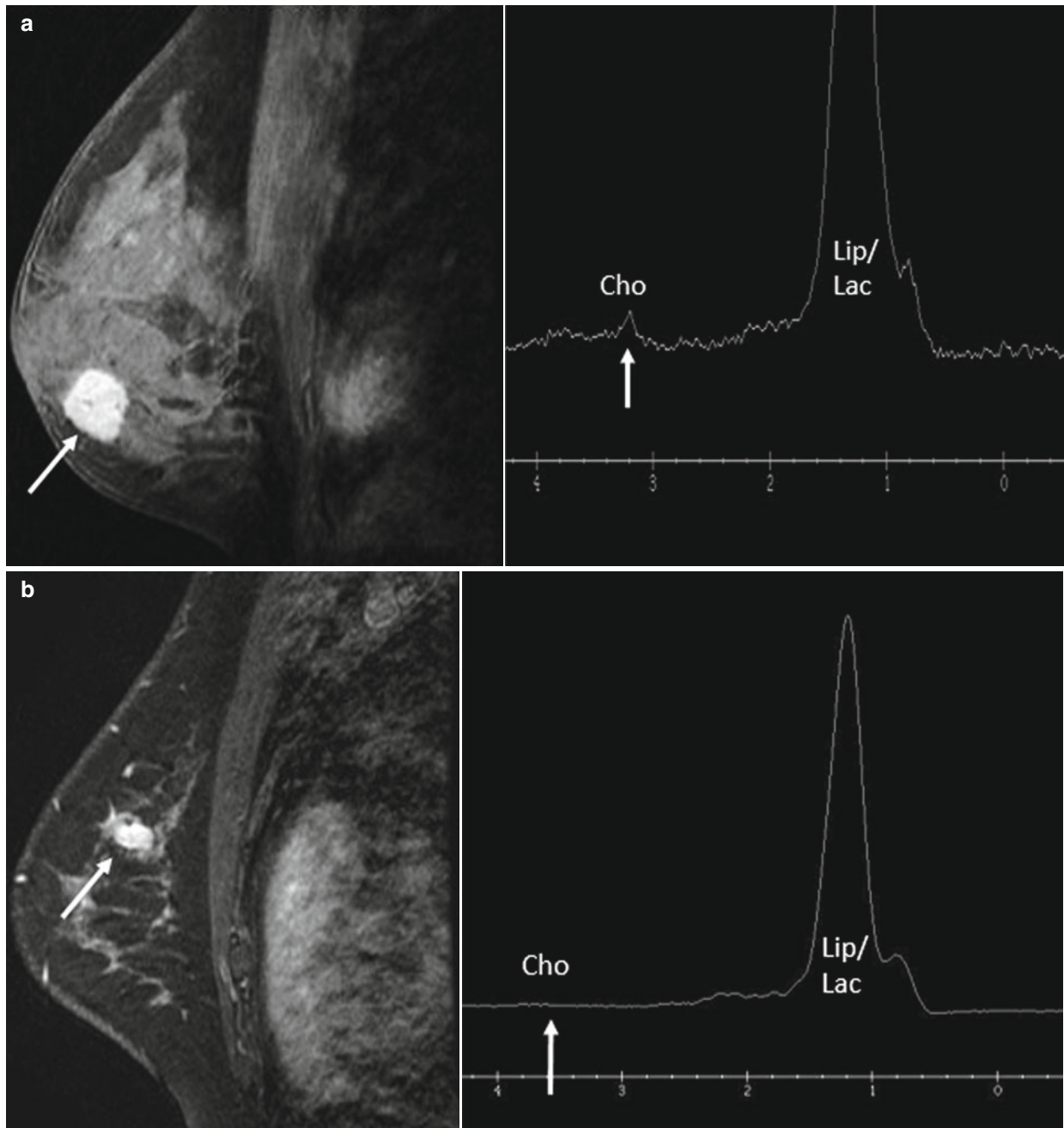
Fig. 19.11 Examples of MR spectroscopy (MRS). (**a**) The malignant mass shown on conventional post-contrast MR image on *left* (*arrow*) displays an elevated choline peak (*right*, *arrow*) when interrogated by MRS. (**b**) The fibroadenoma outlined on post-contrast MR image (*left*, *arrow*) shows no elevation in choline spectral peak (*right*, *arrow*), in keeping with its benign nature. *Lip/Lac* lipid/lactate (Images courtesy of Sunitha B. Thakur, PhD)

Each of these may occur in cancer. As a result, the free motion of water is restricted compared to adjacent normal tissue. This process can be quantified, referred to as the apparent diffusion coefficient (ADC), and can be mapped to allow correlation to standard images of the breast (Fig. 19.12). Many studies have confirmed that the ADC values differ between malignant and benign lesion, with ADCs tending to be lower in cancers (likely related mainly to dense cellularity) [59, 60]. Partridge and associates showed that low ADC was a significant predictor of malignancy and that even when a relatively high discriminating ADC threshold was set so as to allow 100 % sensitivity, biopsy could have been avoided in 33 % of benign cases. Very importantly, that group demonstrated that the improved PPV was realized for non-mass
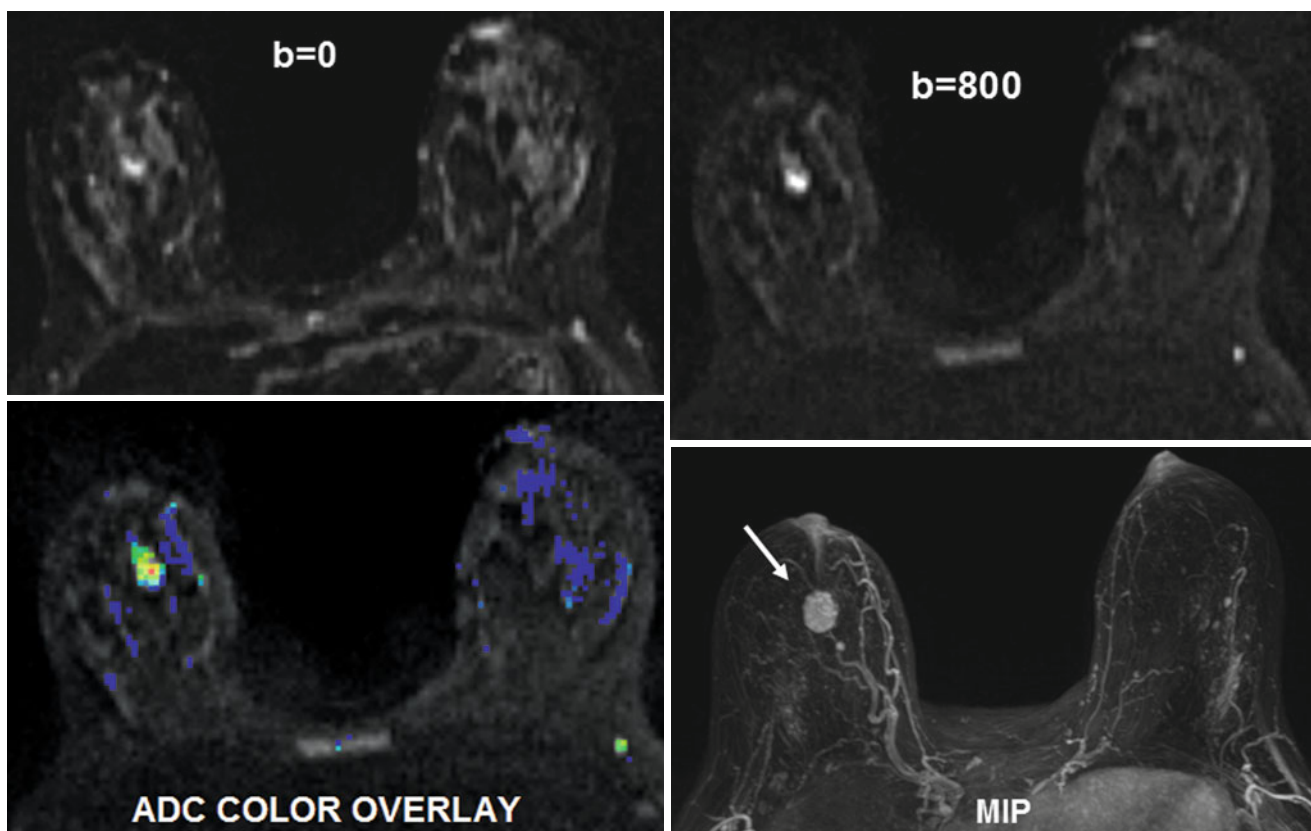
Fig. 19.12 Diffusion-weighted imaging. The cancer seen on the MIP imaged (*lower right*, *arrow*) can be visualized on the DWIs (*top images*) obtained at b values of 0 and 800. Average ADC (1.0 in this case, *low*) is calculated for area of interest, and values are qualitatively displayed by color map (*lower left*) (*red* low ADC) (Courtesy of Hologic®)

lesions and lesions <1 cm, a weakness for MRS [61]. Pinker and associates developed an interpretation system that combined BIRADS features with ADC values. They set ADC discriminator thresholds and used those to potentially modify BIRADS final assessments. For example, if a mass was assigned BIRADS 4 assessment based on morphology and kinetics, but had and ADC >1.39, it was reassigned as a BIRADS 2 lesion. Conversely, a BIRADS 3 lesion could be upgraded if it had an ADC less than the threshold value. Using this system, the group maintained the high sensitivity of standard MRI but improved specificity to 89.4 % [62].

DWI may allow early detection of treatment response to NAC. Several studies have shown that ADC values rise as tumors respond to treatment, often before a change in tumor size is noted and as early as 3 weeks after the start of therapy [63–65]. This likely reflects a change in cell density as tumor dies. DWI may also be able to predict the presence of an invasive component when DCIS is evaluated with MRI. Mori and colleagues showed a statistical difference between the ADC of invasive disease and surrounding DCIS, outlining an invasive nest as small as 1.5 mm [66]. Other exciting work suggests that axillary nodal metastasis detection may eventually become noninvasive. Two groups have found that ADC values between normal nodes and malignant nodes differ significantly [67, 68]. Unfortunately, the groups differed regarding whether involved nodes displayed an increased or decreased ADC compared to normal nodes. This brings to light some important limitations regarding DWI. There is overlap in ADC values between benign and malignant lesions. No absolute discriminatory ADC values have been identified; values identified in the literature appear investigator specific. Additionally, due to poor spatial resolution (related in part to slice thickness), tumor conspicuity as on DWI images suffers compared to standard MRI. These issues will likely be solved, especially with increasing penetration of 3 T units in the market, and DWI is expected to become a routine component of breast MRI evaluation in the near future, with software analytic tools currently available on several dedicated breast MRI interpretation systems.

Other potential technical advances related to MRI are undergoing current evaluation. Tumor micro-vascularity, qualitatively (lesion enhancement morphology) and semiquantitatively (kinetic curves) assessed during routine MR imaging, can be examined more quantitatively, by measuring parameters such as vascular permeability (k^{trans}), the capacity of tissue to absorb contrast (v_e), and flux of contrast within tissue (k_{ep}). Each of

these perfusion parameters reflects the presence of tumor neo-angiogenesis, the new, abnormal vessels that form with cancers. There is much interest in using this information to predict the presence of invasion in lesions thought to be pure DCIS, tumor grade and subtype, and prognostic information noninvasively. For example, Koo and associates found that these parameters could predict tumors with poor prognostic features as defined by tumor markers (estrogen receptor and her-2-neu) [69]. This perfusion work is ongoing and currently the results have not reached consensus, but one can see the progressive refinement of noninvasive measures that will allow increasing personalized tumor detection, prognosis, and treatment assessment. While some of this work is possible at 1.5 T, it is likely that use of 3 T units will allow more robust advancement in these technologies, related to improved temporal and spatial resolution and improved signal-to-noise ratio [70].

Breast-Specific Gamma Imaging

Breast-specific gamma imaging (BSGI), also known as molecular breast imaging (MBI) or breast scintigraphy, is an imaging modality which capitalizes on physiologic differences between breast cancer and normal tissue in order to allow for the detection of neoplasm (Fig. 19.13). The most widely used radiotracer is Tc-99 m sestamibi, which localizes within mitochondria. It is thought that both the higher concentration of mitochondria within cancer cells and the increased delivery of the radiotracer to the tumors because of neovascularity lead to greater uptake of Tc-99 m sestamibi within the cancers relative to the surrounding normal breast tissue. As physiologic, rather than anatomic, characteristics of the breast are imaged, BSGI is postulated to overcome several limitations confounding the interpretation of mammograms including high breast density, postoperative scarring, and breast implants [71].
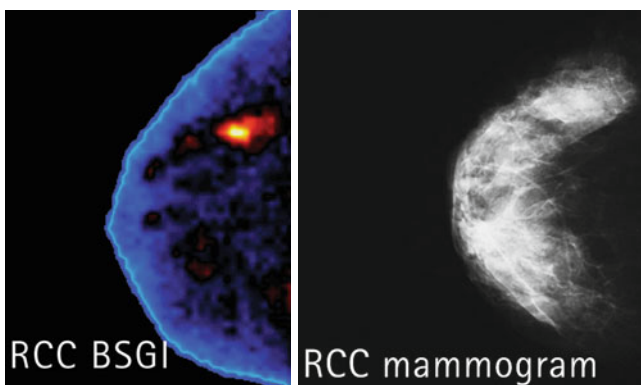

Fig. 19.13 BSGI image demonstrates multiple areas of uptake in the right breast, representing multicentric lobular carcinoma. Mammogram (CC view) demonstrates dense tissue, without abnormality (Images courtesy of Dilon Technologies)

BSGI has its origins in what is known as scintimammography, which used a traditional gamma camera and imaged the patient prone in the lateral and AP positions. This technique was limited in its ability to detect subcentimeter lesions due to the poor resolution of the cameras as well as the inability to position the detector close to the breast [72]. Current gamma imaging employs a high-resolution gamma camera which images the slightly compressed breast in the craniocaudal and mediolateral oblique positions, as is done in mammography. 15–25 mCi of Tc-99 m sestamibi (or, less frequently, Tc-99 m tetrofosmin) are injected, and each image is obtained to 100,000 counts, for a total of approximately 45 min per exam. With the high-resolution camera, the sensitivity for the detection of subcentimeter lesions has improved [73]. Another benefit of the breast-specific gamma camera is that the breast can be imaged in positions comparable to those used in mammography, so that direct correlation between the two imaging modalities can be made [74]. In the past, if a suspicious abnormality was identified on a BSGI examination, second review of the mammogram, directed ultrasound, or MRI were used to attempt to identify the abnormality for targeting for biopsy. Today, a gamma-guided stereotactic localization device is available [71].

BSGI has shown promising results. Brem et al. [75] found that BSGI had a high sensitivity (96.4 %) and a moderate specificity (59.5 %) in a study of 146 patients. This result was echoed in a larger, multicenter trial by Weigert et al. [76] of 1,042 patients which found that gamma imaging had an overall sensitivity of 91 % and a specificity of 77 %. A recent meta-analysis of studies investigating BSGI again concluded that it has a high sensitivity (95 %) and moderate specificity (80 %) [77].

Many believe that BSGI can be a useful imaging modality in patients with dense breasts in whom mammography is known to be of decreased sensitivity. In a study of BSGI as an adjunct to mammography in 936 women with dense breasts, the sensitivity of both modalities combined was significantly higher than that of mammography alone (91 % vs. 27 %), and most detected cancers were node negative [78]. Kim et al. found that gamma imaging was able to detect more additional sites of cancer than mammography in 28/121 women with dense breasts and cancer (83.1 % vs. 44.1 % sensitivity) [79]. Studies suggest that BSGI can be useful in detecting ductal carcinoma in situ (DCIS). In a study of 22 cases, BSGI demonstrated statistically equivalent sensitivity (91 %) for the detection of DCIS when compared to mammography (82 %) and MRI (88 %) [73]. Another study of 33 women demonstrated that BSGI had an equal sensitivity to mammography for the detection of DCIS (93.9 % vs. 90.9 %), but better assessed the extent of disease when correlation with histopathology was done [80]. BSGI has also been shown to be at least as effective in the detection of invasive lobular carcinoma (ILC) as mammography, ultrasound, and MRI. Brem et al. [74] found in a study of 28 lesions that

the sensitivity of BSGI for detecting ILC was 93 %, as compared to 83 % with MRI, 79 % with mammography, and 68 % with ultrasound, though the differences were not statistically significant.

Several studies have compared the utility of BSGI and MRI as adjuncts to mammography. In a study of 33 mammographically indeterminate lesions evaluated both by BSGI and MRI, BSGI was found to have an equal sensitivity to MRI (89 % vs. 100 %, not statistically significant), but a higher specificity (71 % vs. 25 %) [81]. The results of a study of 66 patients with known cancer comparing BSGI to MRI echo these findings of equal sensitivity (88.8 % vs. 92.3 %) and higher specificity (90.1 % vs. 39 %) [82]. One advantage of BSGI over MRI is that it can be used in patients with contraindications to MRI, such as pacemakers, defibrillators, or aneurysm clips, and in patients with claustrophobia who cannot tolerate MRI. Additionally, the potentially hazardous use of gadolinium in patients with renal disease can be avoided. Another advantage is that the number of images generated by BSGI, generally 4–16, is much less than the sometimes thousands of images produced by an MRI, thus not placing such a high burden on storage space and potentially decreasing image interpretation time [71].

Thus, there are many studies that support the use of BSGI as a tool for the detection of breast cancer. However, a limitation of these data is that most of the studies that have been published to date have small sample sizes and are retrospective. More prospective studies with large sample sizes showing the effectiveness of BSGI must be performed before this modality is accepted into mainstream practice. In the end, however, the most critical limitation of BSGI that must be considered is its very high radiation exposure when compared to mammography. Not only is the radiation exposure of BSGI much higher, but the effects are not limited to the breasts as in the case of mammography, as the biodistribution of the tracer throughout the body exposes many organs and tissues to the radiation [83]. It is estimated that at current typical doses, a single BSGI study is associated with a fatal radiation-induced cancer risk comparable to that of a lifetime of annual screening mammography in women starting at age 40 [84]. Therefore, at current doses, it is difficult to support the widespread use of BSGI.

Positron Emission Tomography/Positron Emission Mammography

As mammography, ultrasound and MRI are not without limitations, there has been interest in the use of alternative modalities for the detection and staging of breast cancer. Fluorine-18 (^{18}F) fluorodeoxyglucose (FDG) positron emission tomography (PET) is one such modality. ^{18}F-FDG is a structural glucose analogue that is taken up by and trapped within cells. The more metabolically active the cell, the greater the glucose requirement, and therefore the greater the accumulation of FDG within. Labeling with the positron emitter fluorine-18 allows detection, localization, and quantification of FDG accumulation by PET instrumentation [85]. PEt allows for visualization of tumors based on physiologic, and not anatomic, factors. Therefore, it is not limited by breast density, as in the case of mammography. It also overcomes several limitations imposed by MRI, as it can be performed in patients with claustrophobia, poor renal function, and implanted metal devices and is not affected by hormonal status [86]. Additionally, it allows for whole-body imaging, facilitating staging of malignancy. Its combination with CT permits specific anatomic localization of FDG accumulation [87].

However, PET is not without significant limitations. Most studies have found whole-body PET with or without CT to be of lower utility than MRI in the detection of primary breast tumors. Though in a study by Heusner et al., PET/CT had a statistically equivalent sensitivity for the detection of primary cancers when compared to MRI, MRI was better able to classify the T stage [87]. Most other studies have found a poor performance of whole-body PET in the detection of primary tumor. Choi and colleagues calculated a sensitivity of 89.6 % for PET/CT in detecting the primary lesion, compared to 99.4 % for ultrasound and 98.5 % for MRI [88]. They found that this low sensitivity of PET/CT in detecting the primary tumor was dependent on size—though it was able to detect all T2 or larger cancers, it detected only 81 % of T1 lesions and only 70.8 % of 1 cm or smaller cancers. Avril et al. [89] found that whole-body PET was unable to detect any tumor smaller than 0.5 cm. Sensitivity only increased to 12.5 % for lesions 0.5–1.0 cm in size. For stage T2 tumors, sensitivity increased to 80.6–91.9 %.

Several studies also demonstrate the limitations of whole-body PET in determining the extent of disease in the breast. Though the Heusner et al. study [87] found that PET/CT was better able to correctly classify the focality pattern of lesions when compared to MRI, another study [88] found PET/CT to be a poor detector of multifocality, with a sensitivity of 12.5 % compared to 80.0 % (US) and 81.1 % (MRI). Uematsu et al. [90] also found that PET was significantly less accurate in evaluating tumor extent when compared to MRI (43.5 % vs. 91 %). PET/CT has also been found to be of relatively low utility for staging the axilla, with a mean sensitivity of 63 % [87, 88, 90–93]. This is comparable to the sensitivity of clinical exam, ultrasound, and MRI [87, 88, 92, 93]. As the sensitivity is lower than that of sentinel node biopsy, it cannot be used as a substitute [93].

Many groups have attempted to determine whether the degree of FDG uptake in tumors can be used as a prognostic indicator, but results are conflicting. Several studies [94–98] agree that tumors expressing more Ki-67 have a greater FDG
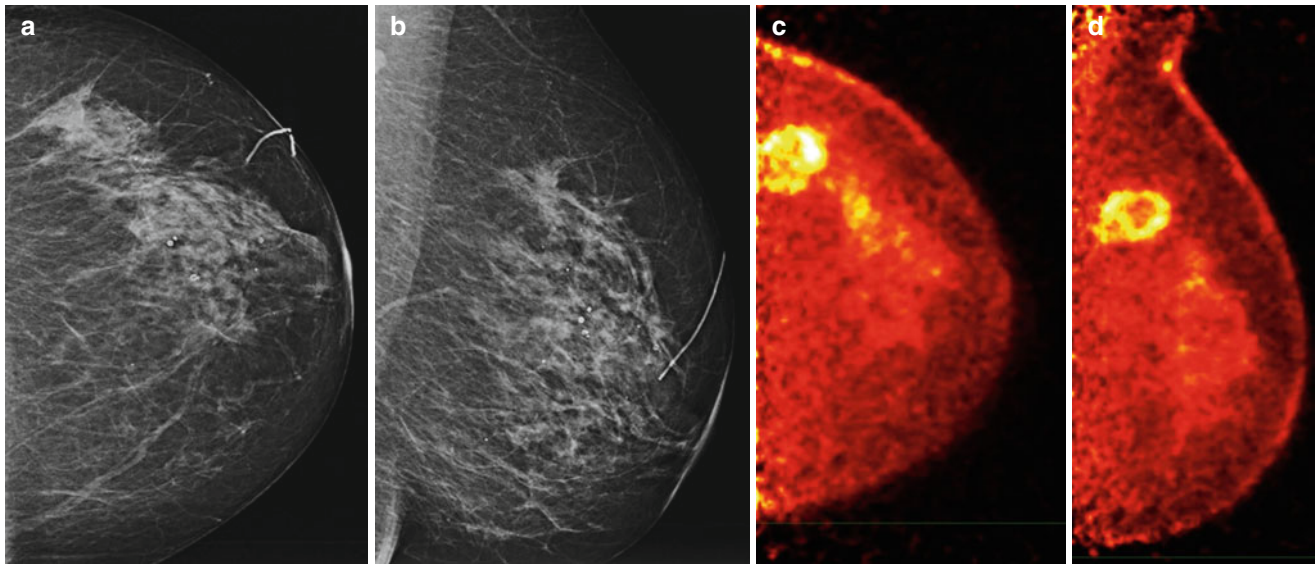
Fig. 19.14 CC (**a**) and MLO mammographic (**b**) views demonstrate no abnormality. Corresponding PEM images (**c, d**) show uptake in the upper outer quadrant, representing invasive lobular carcinoma (Images courtesy of Kathy Schilling, MD)

uptake. Some studies have found that tumors with ductal histology have a higher FDG uptake than those with lobular [94–96, 99] though others [97, 98] have found no correlation between FDG uptake and histology. Similarly, there are conflicting data regarding the association between FDG uptake and tumor size, histological grade, axillary lymph node status, and hormone receptor positivity [94–101]. At least two investigators have found an association between triple negativity and increased FDG uptake [99, 102]. Another found that patients with tumors that had high FDG uptake had a significantly poorer prognosis than those whose tumors had low uptake [101]. One study attempted to determine what tumor characteristics were associated with a false-negative PET [103]. It found that tumor size (less than or equal to 10 mm) and low tumor grade were associated with a false-negative result.

The utility of whole-body PET in breast cancer diagnosis appears to be not in the evaluation of the breast and axilla, but rather, in combination with CT, for the detection of distant metastatic disease. The sensitivity and specificity of PET/CT for detecting distant metastases is much higher than that of conventional imaging (100 and 96.4–98 % vs. 60–61.5 and 83–99.2 %) [88, 91]. This detection of unexpected sites of metastatic disease by PET/CT led to a change in the initial staging in 8–42 % of patients in multiple studies [91, 92, 104]. Whether the detection of these additional sites of disease leads to improved patient survival is yet to be seen. Current recommendations are to use PET in combination with CT [85] in those with clinically suspected metastatic disease. PET/CT has also been found to be useful in the evaluation of patients with recurrent breast cancer. Aukema et al. found that PET/CT changed the clinical management in almost half the patients with tumor recurrence when compared to evaluation with conventional staging procedures (physical examination, MRI, chest radiograph, liver US or CT, and bone scan) [105]. Only one metastasis detected by conventional imaging was missed by PET/CT and was determined to have no clinical consequence for the patient. The authors suggest that PET/CT may replace conventional staging procedures in the future.

Positron emission mammography (PEM), or breast PET, was developed in order to take advantage of PET's benefits in detecting breast cancer (e.g. not being dependent on breast density or hormonal status) while overcoming its limitations, specifically its low sensitivity for small cancers [106]. This is thought to be possible because the dedicated PEM cameras are small and are able to be positioned closer to the breast, and also use compression, which reduces the effects of motion [107]. PEM uses two parallel photon detectors that are positioned on the breast similar to a mammography unit [108]. Initial studies showed that PEM could be effective in identifying breast cancers (Fig. 19.14a–d). One study of 18 lesions demonstrated that PEM had a sensitivity of 86 %, specificity of 91 %, and overall diagnostic accuracy of 89 % [109]. Another pilot study of 23 patients also demonstrated a sensitivity of 86 % and demonstrated that PEM can be effective in finding cancers as small as 4 mm [110]. A third preliminary study of 44 women with known breast cancer found that most index cancers (39/44 or 89 %) could be seen with PEM, while PEM was also able to detect three incidental cancers not seen by any other modality. This study also found that PEM could be effective in predicting margin status, as out of 19 patients who underwent breast-conserving surgery, PEM correctly predicted 6/8 (75 %) with positive margins and 11/11 (100 %) of those with negative margins [111].

Larger studies confirm these results. A study of 94 patients with known or suspected cancers found that PEM had a sensitivity of 90 % and specificity of 86 % [112].

Compared to whole-body PET, PEM is able to see smaller cancers. PEM was found to be more sensitive than PET/CT in the detection of cancer, and the difference in sensitivity was accentuated in small tumors [108]. A pilot study found a cancer as small as 4 cm [110]. Berg et al. found that PEM had a sensitivity of 63 % for cancers smaller than 1 cm [106]. In a large series of 472 patients with newly diagnosed breast cancer, Berg et al. [112, 113] compared the performance of PEM with that of MRI in detecting cancer in the ipsilateral and contralateral breasts. When evaluating the ipsilateral breast, MRI was found to have greater lesion-level sensitivity for additional malignant lesions (53 % vs. 47 %) and to more accurately predict the need for mastectomy, though breast-level sensitivity was comparable. PEM was found to have greater specificity (79.9 % vs. 65.6 %). In the contralateral breast, sensitivity of PEM for cancer detection was lower than that of MRI (73 % vs. 93 %). Another study [86] comparing PEM with MRI found that they had the same index lesion depiction sensitivity (92.8 %), greater than whole-body PET (67.9 %). Similarly, there was no significant difference between PEM and MRI in the detection of additional unsuspected lesions.

One limitation of PEM is that the far posterior portion of the breast may not be adequately imaged due to limited coincidence-count sampling at the edge, as well as detector plates excluding the far posterior breast from the field of view. One study found that all three false-negative cases (out of 20 total cases) were of cancers located in the posterior breast [110]. Another significant limitation of PEM is that it employs ionizing radiation. It is estimated that at current typical doses, a single PEM study is associated with a fatal radiation-induced cancer risk comparable to that of a lifetime of annual screening mammography in women starting at age 40 [84]. Therefore, given the evidence that it is, at best, comparable to MRI in detecting breast cancer, PEM is unlikely to be widely accepted as the preferred study in patients able to undergo MRI examinations.

Optical Imaging

The use of light for the detection and characterization of breast cancer is appealing on many levels. It uses no ionizing radiation, does not require significant breast compression and can provide functional information. Max Cutler used optical imaging (OI) in its most basic form in the 1920s when he transilluminated the breast in an attempt to outline and characterize pathology [114]. Dr. Cutler applied a narrow-beam light source to the undersurface of the flattened breast of a seated patient and observed from above. He noted that the various

tissues encountered in the breast differentially transmitted or absorbed light. Fatty tissue and cysts were translucent, while solid masses and anything containing hemorrhagic material were "intensely opaque." He evaluated palpable masses and felt he could differentiate simple cysts (which he recognized as clinically unimportant) from hemorrhagic cysts and solid masses (clinically important). Additionally, he used transillumination technique to evaluate bloody nipple discharge and was able to identify and localize papillomas in some cases, thereby precluding the need for mastectomy, which was sometimes the treatment for suspicious nipple discharge in that period. However, despite Dr. Cutler's enthusiasm, the technique did not gain a foothold. In the 1970s and 1980s, interest was revived, using improved technology consisting of a near-infrared (NIR) light source and dedicated detectors, as the human eye is insensitive to NIR light. The literature surrounding this technique was largely anecdotal but claimed some success. When scrutinized in a more methodological manner, it was found wanting, detecting only 53 % of cancers present in a study population of 1,239 women compared to 96 % found with mammography and only 19 % of subclinical and small (<1 cm) cancers [115].

Given its theoretical appeal, however, experimentation with the technology continued, with resultant emergence of more sophisticated methods of transmitting and receiving NIR light as well as interrogation of more physiologic and functional tissue attributes, over and above simple light transmission versus absorption. Some of these improvements included development of diffuse optical tomography (DOT), which sends laser-generated NIR light into the breast in multiple projections and, using mathematical reconstruction, can create a 3D map of the breast. Traditional tissue absorption information is obtained. However, additionally, when light of varying frequencies is delivered, spectroscopic data can be ascertained. Some of the main "chromophores" (tissue absorbers) in the breast include oxyhemoglobin, deoxyhemoglobin, water, and lipid, and via their unique and quantifiable spectroscopic footprint, they can be mapped within the breast. Each of these chromophores has an implication in tissue metabolism, neoangiogenesis, necrosis, and extracellular water content and thus the presence, etiology, and status of a breast tumor.

A comprehensive review of the clinical data surrounding breast optical imaging was performed by Leff and colleagues [116]. They concluded that the technique allows lesion detection in 85 % of cases, due mainly to increased concentrations of tissue oxyhemoglobin (reflecting neovascularity) and deoxyhemoglobin (indicative of tissue metabolism). It underperforms in detecting small cancers (due to poor spatial resolution). Importantly, they observed that the data do not convincingly demonstrate the ability of optical imaging to differentiate between benign and malignant lesions. Given these data, when combined with non-superior sensitivity, they concluded that in its current form optical
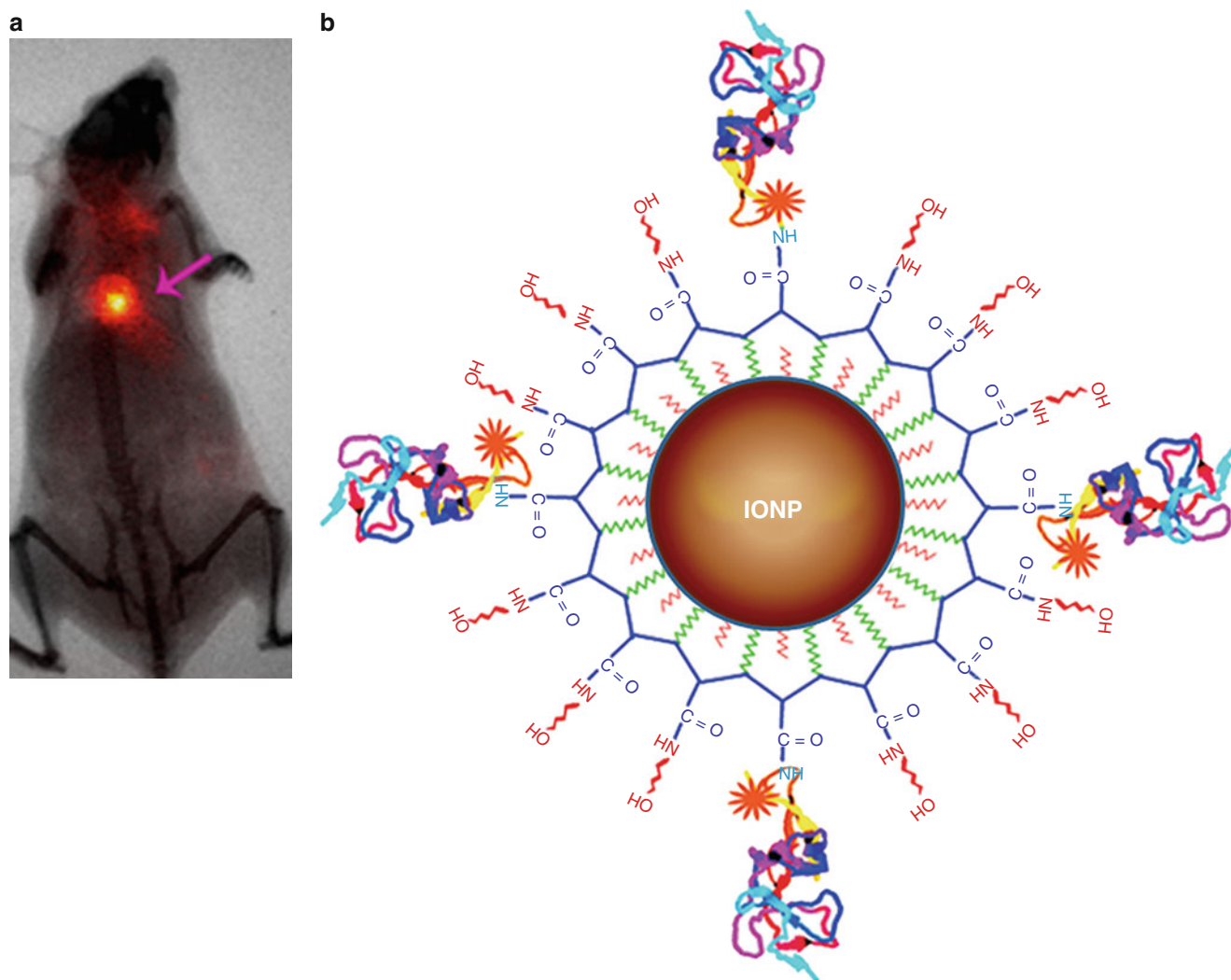
a   **b**

Fig. 19.15 (**a**) NIR optical imaging. 4T1 mouse mammary tumor model. Fluorescent dye attached to a nanoparticle is injected intravenously and concentrates selectively (*outlined by arrow*) in a mammary tumor in this mouse. It is activated by near-infrared light and can be imaged. The nanoparticle, displayed schematically (**b**), can be made tumor specific and may also be bound to chemotherapeutic agents, creating a "theranostic" particle [122]. *IONP* Iron oxide nanoparticles (Images courtesy of Lily Yang, MD, PhD)

imaging cannot supplant mammography, but with further refinement, may play a part in multimodality breast imaging in certain scenarios. For example, Soliman et al. showed that optical imaging may be a useful, noninvasive, relatively inexpensive way to determine response to neoadjuvant chemotherapy in patients with locally advanced breast cancer as early as 4 weeks into treatment [117].

Exciting new refinements are currently being evaluated. Fluorescent dyes are being explored as way to improve sensitivity and specificity. These cyanine-based dyes are administered intravenously and collect in neoplastic tissue, related to leaky tumor vascularity, similar to MRI and CT contrast material. Not only do they act as NIR light absorbers when concentrated within tumors (just as oxy- and deoxyhemoglobin, lipid, and water do), but they also fluoresce when excited by external application of NIR light, allowing detection and

localization by an optical imaging tomographic unit. In a multicenter clinical trial, Poellinger and associates [118] confirmed potential clinical utility for this technology, noting 100 % sensitivity for cancer detection at certain administered doses of this dye in a dose-escalating design study. However, they also noted that sensitivity was related to dose, lesion size, breast size, and lesion depth, with overall sensitivity of 60.9 % for invasive cancers. Additionally, the optimal imaging dose they defined was far different from that determined by other authors [119], suggesting that this work is still in its developmental stages. Other related, potentially "game-changing" work is undergoing in vivo evaluation on an animal level. In this work, fluorescent dyes are being made tumor specific by attaching estrogen [120] or Her2-targeted Affibody molecules [121] (Fig. 19.15a, b). Since these molecules/nanoparticles (the number and type of which will

likely be expanded rapidly as more is discovered about tumor-specific surface and intracellular markers) would be expected to attach specifically to primary cancers and metastases, and not to normal cells, the specter of tailored detection and tumor monitoring is easily imagined. With the addition of a chemotherapeutic agent to the nanoparticle (rendering it "theranostic"), as has been developed by Shalviri and colleagues [122], highly tailored therapy is added to the mix, potentially markedly diminishing the debilitating systemic effects of treatment, as only the cancer is being targeted and not healthy tissue.

Conclusion

The exciting new technologies outlined previously will likely allow for improved sensitivity and specificity in breast cancer detection and lesions characterization. However, the field of breast imaging finds itself at an unusual crossroads. On one hand, there is pressure, even from politicians and the public, to image more, especially in populations deemed to be at elevated risk. On the other hand, many of our tools have been accused of leading to overdiagnosis, mental anguish in patients, unnecessary added interventions, and cost run-ups. It seems prudent to move forward with technological developments and research, rather than retreat, with the goal of further refining our tools so that they can be applied appropriately, even if sometimes selectively, to maximize outcomes benefit.

References

1. Niklason LT, Christian BT, Niklason LE, Kopans DB, Castleberry DE, Opsahl-Ong BH, et al. Digital tomosynthesis in breast imaging. Radiology. 1997;205(2):399–406.
2. FDA. Selenia Dimensions 3D System- P080003. 2011 [updated 20 May 2013; cited 05 Jun 2013]. Available from: http://www.fda.gov/MedicalDevices/ProductsandMedicalProcedures/DeviceApprovalsandClearances/Recently-ApprovedDevices/ucm246400.htm.
3. Waldherr C, Cerny P, Altermatt HJ, Berclaz G, Ciriolo M, Buser K, et al. Value of one-view breast tomosynthesis versus two-view mammography in diagnostic workup of women with clinical signs and symptoms and in women recalled from screening. AJR Am J Roentgenol. 2013;200(1):226–31.
4. Svahn TM, Chakraborty DP, Ikeda D, Zackrisson S, Do Y, Mattsson S, et al. Breast tomosynthesis and digital mammography: a comparison of diagnostic accuracy. Br J Radiol. 2012;85(1019):e1074–82.
5. Teertstra HJ, Loo CE, van den Bosch MA, van Tinteren H, Rutgers EJ, Muller SH, et al. Breast tomosynthesis in clinical practice: initial results. Eur Radiol. 2010;20(1):16–24.
6. Gennaro G, Toledano A, di Maggio C, Baldan E, Bezzon E, La Grassa M, et al. Digital breast tomosynthesis versus digital mammography: a clinical performance study. Eur Radiol. 2010;20(7):1545–53.
7. Skaane P, Bandos AI, Gullien R, Eben EB, Ekseth U, Haakenaasen U, et al. Comparison of digital mammography alone and digital mammography plus tomosynthesis in a population-based screening program. Radiology. 2013;267(1):47–56.
8. Rafferty EA, Park JM, Philpotts LE, Poplack SP, Sumkin JH, Halpern EF, et al. Assessing radiologist performance using combined digital mammography and breast tomosynthesis compared with digital mammography alone: results of a multicenter, multireader trial. Radiology. 2013;266(1):104–13.
9. Poplack SP, Tosteson TD, Kogel CA, Nagy HM. Digital breast tomosynthesis: initial experience in 98 women with abnormal digital screening mammography. AJR Am J Roentgenol. 2007;189(3):616–23.
10. Gur D, Abrams GS, Chough DM, Ganott MA, Hakim CM, Perrin RL, et al. Digital breast tomosynthesis: observer performance study. AJR Am J Roentgenol. 2009;193(2):586–91.
11. Rose SL, Tidwell AL, Bujnoch LJ, Kushwaha AC, Nordmann AS, Sexton Jr R. Implementation of breast tomosynthesis in a routine screening practice: an observational study. AJR Am J Roentgenol. 2013;200(6):1401–8.
12. Brandt KR, Craig DA, Hoskins TL, Henrichsen TL, Bendel EC, Brandt SR, et al. Can digital breast tomosynthesis replace conventional diagnostic mammography views for screening recalls without calcifications? A comparison study in a simulated clinical setting. AJR Am J Roentgenol. 2013;200(2):291–8.
13. Noroozian M, Hadjiiski L, Rahnama-Moghadam S, Klein KA, Jeffries DO, Pinsky RW, et al. Digital breast tomosynthesis is comparable to mammographic spot views for mass characterization. Radiology. 2012;262(1):61–8.
14. Zuley ML, Bandos AI, Ganott MA, Sumkin JH, Kelly AE, Catullo VJ, et al. Digital breast tomosynthesis versus supplemental diagnostic mammographic views for evaluation of noncalcified breast lesions. Radiology. 2013;266(1):89–95.
15. Wallis MG, Moa E, Zanca F, Leifland K, Danielsson M. Two-view and single-view tomosynthesis versus full-field digital mammography: high-resolution X-ray imaging observer study. Radiology. 2012;262(3):788–96.
16. Spangler ML, Zuley ML, Sumkin JH, Abrams G, Ganott MA, Hakim C, et al. Detection and classification of calcifications on digital breast tomosynthesis and 2D digital mammography: a comparison. AJR Am J Roentgenol. 2011;196(2):320–4.
17. FDA. Selenia Dimensions 3D System – P080003/S001 2013 [updated 23 May 2013; cited 20 Jun 2013]. Available from: http://www.fda.gov/MedicalDevices/ProductsandMedicalProcedures/DeviceApprovalsandClearances/Recently-ApprovedDevices/ucm353734.htm.
18. D'Orsi CJ, Getty DJ, Pickett RM, Sechopoulos I, Newell MS, Gundry KR, et al. Stereoscopic digital mammography: improved specificity and reduced rate of recall in a prospective clinical trial. Radiology. 2013;266(1):81–8.
19. Dromain C, Thibault F, Muller S, Rimareix F, Delaloge S, Tardivon A, et al. Dual-energy contrast-enhanced digital mammography: initial clinical results. Eur Radiol. 2011;21(3):565–74.
20. Lewin JM, Niklason L. Advanced applications of digital mammography: tomosynthesis and contrast-enhanced digital mammography. Semin Roentgenol. 2007;42(4):243–52.
21. Jochelson MS, Dershaw DD, Sung JS, Heerdt AS, Thornton C, Moskowitz CS, et al. Bilateral contrast-enhanced dual-energy digital mammography: feasibility and comparison with conventional digital mammography and MR imaging in women with known breast carcinoma. Radiology. 2013;266(3):743–51.
22. Dromain C, Thibault F, Diekmann F, Fallenberg EM, Jong RA, Koomen M, et al. Dual-energy contrast-enhanced digital mammography: initial clinical results of a multireader, multicase study. Breast Cancer Res. 2012;14(3):R94.
23. Jong RA, Yaffe MJ, Skarpathiotakis M, Shumak RS, Danjoux NM, Gunesekara A, et al. Contrast-enhanced digital mammography: initial clinical experience. Radiology. 2003;228(3):842–50.
24. Diekmann F, Diekmann S, Taupitz M, Bick U, Winzer KJ, Huttner C, et al. Use of iodine-based contrast media in digital full-field mammography–initial experience. Rofo. 2003;175(3):342–5.

25. Diekmann F, Freyer M, Diekmann S, Fallenberg EM, Fischer T, Bick U, et al. Evaluation of contrast-enhanced digital mammography. Eur J Radiol. 2011;78(1):112–21.

26. Dromain C, Balleyguier C, Muller S, Mathieu MC, Rochard F, Opolon P, et al. Evaluation of tumor angiogenesis of breast carcinoma using contrast-enhanced digital mammography. AJR Am J Roentgenol. 2006;187(5):W528–37.

27. Lewin JM, Isaacs PK, Vance V, Larke FJ. Dual-energy contrast-enhanced digital subtraction mammography: feasibility. Radiology. 2003;229(1):261–8.

28. Dodd GD. Present status of thermography, ultrasound and mammography in breast cancer detection. Cancer. 1977;39(6 Suppl): 2796–805.

29. Kobayashi T, Takatani O, Hattori N, Kimura K. Differential diagnosis of breast tumors. The sensitivity graded method ultrasonotomography and clinical evaluation of its diagnostic accuracy. Cancer. 1974;33(4):940–51.

30. Graf O, Helbich TH, Hopf G, Graf C, Sickles EA. Probably benign breast masses at US: is follow-up an acceptable alternative to biopsy? Radiology. 2007;244(1):87–93.

31. Stavros AT. Breast ultrasound. Philadelphia: Lippincott Williams & Williams; 2004.

32. Berg WA, Blume JD, Cormack JB, Mendelson EB, Lehrer D, Bohm-Velez M, et al. Combined screening with ultrasound and mammography vs mammography alone in women at elevated risk of breast cancer. JAMA. 2008;299(18):2151–63.

33. Tohno E, Ueno E, Watanabe H. Ultrasound screening of breast cancer. Breast Cancer. 2009;16(1):18–22.

34. Corsetti V, Ferrari A, Ghirardi M, Bergonzini R, Bellarosa S, Angelini O, et al. Role of ultrasonography in detecting mammographically occult breast carcinoma in women with dense breasts. Radiol Med. 2006;111(3):440–8.

35. Kelly KM, Richwald GA. Automated whole-breast ultrasound: advancing the performance of breast cancer screening. Semin Ultrasound CT MR. 2011;32(4):273–80.

36. Wang HY, Jiang YX, Zhu QL, Zhang J, Dai Q, Liu H, et al. Differentiation of benign and malignant breast lesions: a comparison between automatically generated breast volume scans and handheld ultrasound examinations. Eur J Radiol. 2012;81(11): 3190–200.

37. Kelly KM, Dean J, Comulada WS, Lee SJ. Breast cancer detection using automated whole breast ultrasound and mammography in radiographically dense breasts. Eur Radiol. 2010;20(3):734–42.

38. Itoh A, Ueno E, Tohno E, Kamma H, Takahashi H, Shiina T, et al. Breast disease: clinical application of US elastography for diagnosis. Radiology. 2006;239(2):341–50.

39. Sadigh G, Carlos RC, Neal CH, Dwamena BA. Ultrasonographic differentiation of malignant from benign breast lesions: a meta-analytic comparison of elasticity and BIRADS scoring. Breast Cancer Res Treat. 2012;133(1):23–35.

40. Regner DM, Hesley GK, Hangiandreou NJ, Morton MJ, Nordland MR, Meixner DD, et al. Breast lesions: evaluation with US strain imaging–clinical experience of multiple observers. Radiology. 2006;238(2):425–37.

41. Berg WA, Cosgrove DO, Dore CJ, Schafer FK, Svensson WE, Hooley RJ, et al. Shear-wave elastography improves the specificity of breast US: the BE1 multinational study of 939 masses. Radiology. 2012;262(2):435–49.

42. Kashikura Y, Nakayama R, Hizukuri A, Noro A, Nohara Y, Nakamura T, et al. Improved differential diagnosis of breast masses on ultrasonographic images with a computer-aided diagnosis scheme for determining histological classifications. Acad Radiol. 2013;20(4):471–7.

43. Lindfors KK, Boone JM, Newell MS, D'Orsi CJ. Dedicated breast computed tomography: the optimal cross-sectional imaging solution? Radiol Clin North Am. 2010;48(5):1043–54.

44. Kalender WA. Concepts for high-resolution CT of the breast. In: Digital mammography. Berlin/Heidelberg: Springer; 2010. p. 421–7.

45. O'Connell A, Conover DL, Zhang Y, Seifert P, Logan-Young W, Lin CF, et al. Cone-beam CT for breast imaging: radiation dose, breast coverage, and image quality. AJR Am J Roentgenol. 2010; 195(2):496–509.

46. Lindfors KK, Boone JM, Nelson TR, Yang K, Kwan AL, Miller DF. Dedicated breast CT: initial clinical experience. Radiology. 2008;246(3):725–33.

47. Prionas ND, Lindfors KK, Ray S, Huang SY, Beckett LA, Monsky WL, et al. Contrast-enhanced dedicated breast CT: initial clinical experience. Radiology. 2010;256(3):714–23.

48. Kalender WA, Beister M, Boone JM, Kolditz D, Vollmar SV, Weigel MC. High-resolution spiral CT of the breast at very low dose: concept and feasibility considerations. Eur Radiol. 2012;22(1):1–8.

49. McKinley RL, Tornai MP, Tuttle LA, et al. Development and initial demonstration of a low-dose dedicated fully 3-D CT system. In: Maidment ADA, Bakic P, Gavenonis D, editors. Breast imaging. Berlin/Heidelberg: Springer; 2012. p. 442–9.

50. Tozaki M, Fukuma E. 1H MR spectroscopy and diffusion-weighted imaging of the breast: are they useful tools for characterizing breast lesions before biopsy? AJR Am J Roentgenol. 2009; 193(3):840–9.

51. Bolan PJ, Meisamy S, Baker EH, Lin J, Emory T, Nelson M, et al. In vivo quantification of choline compounds in the breast with 1H MR spectroscopy. Magn Reson Med. 2003;50(6):1134–43.

52. Bartella L, Morris EA, Dershaw DD, Liberman L, Thakur SB, Moskowitz C, et al. Proton MR spectroscopy with choline peak as malignancy marker improves positive predictive value for breast cancer diagnosis: preliminary study. Radiology. 2006;239(3): 686–92.

53. Dorrius MD, Pijnappel RM, van der Weide Jansen MC, Jansen L, Kappert P, Oudkerk M, et al. The added value of quantitative multi-voxel MR spectroscopy in breast magnetic resonance imaging. Eur Radiol. 2012;22(4):915–22.

54. Mann RM, Kuhl CK, Kinkel K, Boetes C. Breast MRI: guidelines from the European Society of Breast Imaging. Eur Radiol. 2008;18(7):1307–18.

55. Meisamy S, Bolan PJ, Baker EH, Bliss RL, Gulbahce E, Everson LI, et al. Neoadjuvant chemotherapy of locally advanced breast cancer: predicting response with in vivo (1)H MR spectroscopy–a pilot study at 4 T. Radiology. 2004;233(2):424–31.

56. Tozaki M, Sakamoto M, Oyama Y, Maruyama K, Fukuma E. Predicting pathological response to neoadjuvant chemotherapy in breast cancer with quantitative 1H MR spectroscopy using the external standard method. J Magn Reson Imaging. 2010;31(4): 895–902.

57. Razek NMA. Role of proton MR spectroscopy in high field magnet (3T) in diagnosis of indeterminate breast masses (BIRDS 3 & 4). Egypt J Radiol Nucl Med. 2012;43(4):657–62.

58. McLaughlin R, Hylton N. MRI in breast cancer therapy monitoring. NMR Biomed. 2011;24(6):712–20.

59. Partridge SC, Mullins CD, Kurland BF, Allain MD, DeMartini WB, Eby PR, et al. Apparent diffusion coefficient values for discriminating benign and malignant breast MRI lesions: effects of lesion type and size. AJR Am J Roentgenol. 2010;194(6): 1664–73.

60. Marini C, Iacconi C, Giannelli M, Cilotti A, Moretti M, Bartolozzi C. Quantitative diffusion-weighted MR imaging in the differential diagnosis of breast lesion. Eur Radiol. 2007;17(10):2646–55.

61. Partridge SC, DeMartini WB, Kurland BF, Eby PR, White SW, Lehman CD. Quantitative diffusion-weighted imaging as an adjunct to conventional breast MRI for improved positive predictive value. AJR Am J Roentgenol. 2009;193(6):1716–22.

62. Pinker K, Bickel H, Helbich TH, Gruber S, Dubsky P, Pluschnig U, et al. Combined contrast-enhanced magnetic resonance and diffusion-weighted imaging reading adapted to the "Breast Imaging Reporting and Data System" for multiparametric 3-T imaging of breast lesions. Eur Radiol. 2013;23(7):1791–802.

63. Tozaki M, Oyama Y, Fukuma E. Preliminary study of early response to neoadjuvant chemotherapy after the first cycle in breast cancer: comparison of 1H magnetic resonance spectroscopy with diffusion magnetic resonance imaging. Jpn J Radiol. 2010;28(2):101–9.

64. Manton DJ, Chaturvedi A, Hubbard A, Lind MJ, Lowry M, Maraveyas A, et al. Neoadjuvant chemotherapy in breast cancer: early response prediction with quantitative MR imaging and spectroscopy. Br J Cancer. 2006;94(3):427–35.

65. Nilsen L, Fangberget A, Geier O, Olsen DR, Seierstad T. Diffusion-weighted magnetic resonance imaging for pretreatment prediction and monitoring of treatment response of patients with locally advanced breast cancer undergoing neoadjuvant chemotherapy. Acta Oncol. 2010;49(3):354–60.

66. Mori N, Ota H, Mugikura S, Takasawa C, Tominaga J, Ishida T, et al. Detection of invasive components in cases of breast ductal carcinoma in situ on biopsy by using apparent diffusion coefficient MR parameters. Eur Radiol. 2013;23(10):2705–12.

67. Kamitani T, Hatakenaka M, Yabuuchi H, Matsuo Y, Fujita N, Jinnouchi M, et al. Detection of axillary node metastasis using diffusion-weighted MRI in breast cancer. Clin Imaging. 2013; 37(1):56–61.

68. Luo N, Su D, Jin G, Liu L, Zhu X, Xie D, et al. Apparent diffusion coefficient ratio between axillary lymph node with primary tumor to detect nodal metastasis in breast cancer patients. J Magn Reson Imaging. 2013;38(4):824–8.

69. Koo HR, Cho N, Song IC, Kim H, Chang JM, Yi A, et al. Correlation of perfusion parameters on dynamic contrast-enhanced MRI with prognostic factors and subtypes of breast cancers. J Magn Reson Imaging. 2012;36(1):145–51.

70. Rahbar H, Partridge SC, DeMartini WB, Thursten B, Lehman CD. Clinical and technical considerations for high quality breast MRI at 3 Tesla. J Magn Reson Imaging. 2013;37(4):778–90.

71. Brem RF, Rechtman LR. Nuclear medicine imaging of the breast: a novel, physiologic approach to breast cancer detection and diagnosis. Radiol Clin North Am. 2010;48(5):1055–74.

72. Taillefer R. Clinical applications of 99mTc-sestamibi scintimammography. Semin Nucl Med. 2005;35(2):100–15.

73. Brem RF, Fishman M, Rapelyea JA. Detection of ductal carcinoma in situ with mammography, breast specific gamma imaging, and magnetic resonance imaging: a comparative study. Acad Radiol. 2007;14(8):945–50.

74. Brem RF, Ioffe M, Rapelyea JA, Yost KG, Weigert JM, Bertrand ML, et al. Invasive lobular carcinoma: detection with mammography, sonography, MRI, and breast-specific gamma imaging. AJR Am J Roentgenol. 2009;192(2):379–83.

75. Brem RF, Floerke AC, Rapelyea JA, Teal C, Kelly T, Mathur V. Breast-specific gamma imaging as an adjunct imaging modality for the diagnosis of breast cancer. Radiology. 2008;247(3): 651–7.

76. Weigert JM, Bertrand ML, Lanzkowsky L, Stern LH, Kieper DA. Results of a multicenter patient registry to determine the clinical impact of breast-specific gamma imaging, a molecular breast imaging technique. AJR Am J Roentgenol. 2012;198(1): W69–75.

77. Sun Y, Wei W, Yang HW, Liu JL. Clinical usefulness of breast-specific gamma imaging as an adjunct modality to mammography for diagnosis of breast cancer: a systemic review and meta-analysis. Eur J Nucl Med Mol Imaging. 2013;40(3):450–63.

78. Rhodes DJ, Hruska CB, Phillips SW, Whaley DH, O'Connor MK. Dedicated dual-head gamma imaging for breast cancer screening in women with mammographically dense breasts. Radiology. 2011;258(1):106–18.

79. Kim BS, Moon BI, Cha ES. A comparative study of breast-specific gamma imaging with the conventional imaging modality in breast cancer patients with dense breasts. Ann Nucl Med. 2012;26(10):823–9.

80. Spanu A, Sanna D, Chessa F, Cottu P, Manca A, Madeddu G. Breast scintigraphy with breast-specific gamma-camera in the detection of ductal carcinoma in situ: a correlation with mammography and histologic subtype. J Nucl Med. 2012;53(10):1528–33.

81. Brem RF, Petrovitch I, Rapelyea JA, Young H, Teal C, Kelly T. Breast-specific gamma imaging with 99mTc-Sestamibi and magnetic resonance imaging in the diagnosis of breast cancer–a comparative study. Breast J. 2007;13(5):465–9.

82. Kim BS. Usefulness of breast-specific gamma imaging as an adjunct modality in breast cancer patients with dense breast: a comparative study with MRI. Ann Nucl Med. 2012;26(2):131–7.

83. O'Connor MK, Li H, Rhodes DJ, Hruska CB, Clancy CB, Vetter RJ. Comparison of radiation exposure and associated radiation-induced cancer risks from mammography and molecular imaging of the breast. Med Phys. 2010;37(12):6187–98.

84. Hendrick RE. Radiation doses and cancer risks from breast imaging studies. Radiology. 2010;257(1):246–53.

85. Fletcher JW, Djulbegovic B, Soares HP, Siegel BA, Lowe VJ, Lyman GH, et al. Recommendations on the use of 18F-FDG PET in oncology. J Nucl Med. 2008;49(3):480–508.

86. Schilling K, Narayanan D, Kalinyak JE, The J, Velasquez MV, Kahn S, et al. Positron emission mammography in breast cancer presurgical planning: comparisons with magnetic resonance imaging. Eur J Nucl Med Mol Imaging. 2011;38(1):23–36.

87. Heusner TA, Kuemmel S, Umutlu L, Koeninger A, Freudenberg LS, Hauth EA, et al. Breast cancer staging in a single session: whole-body PET/CT mammography. J Nucl Med. 2008;49(8):1215–22.

88. Choi YJ, Shin YD, Kang YH, Lee MS, Lee MK, Cho BS, et al. The effects of preoperative (18)F-FDG PET/CT in breast cancer patients in comparison to the conventional imaging study. J Breast Cancer. 2012;15(4):441–8.

89. Avril N, Rose CA, Schelling M, Dose J, Kuhn W, Bense S, et al. Breast imaging with positron emission tomography and fluorine-18 fluorodeoxyglucose: use and limitations. J Clin Oncol. 2000;18(20):3495–502.

90. Uematsu T, Kasami M, Yuen S. Comparison of FDG PET and MRI for evaluating the tumor extent of breast cancer and the impact of FDG PET on the systemic staging and prognosis of patients who are candidates for breast-conserving therapy. Breast Cancer. 2009;16(2):97–104.

91. Fuster D, Duch J, Paredes P, Velasco M, Munoz M, Santamaria G, et al. Preoperative staging of large primary breast cancer with [18F]fluorodeoxyglucose positron emission tomography/computed tomography compared with conventional imaging procedures. J Clin Oncol. 2008;26(29):4746–51.

92. Segaert I, Mottaghy F, Ceyssens S, De Wever W, Stroobants S, Van Ongeval C, et al. Additional value of PET-CT in staging of clinical stage IIB and III breast cancer. Breast J. 2010;16(6):617–24.

93. Cooper KL, Harnan S, Meng Y, Ward SE, Fitzgerald P, Papaioannou D, et al. Positron emission tomography (PET) for assessment of axillary lymph node status in early breast cancer: a systematic review and meta-analysis. EurJ Surg Oncol. 2011;37(3):187–98.

94. Gil-Rendo A, Martinez-Regueira F, Zornoza G, Garcia-Velloso MJ, Beorlegui C, Rodriguez-Spiteri N. Association between [18F]fluorodeoxyglucose uptake and prognostic parameters in breast cancer. Br J Surg. 2009;96(2):166–70.

95. Buck A, Schirrmeister H, Kuhn T, Shen C, Kalker T, Kotzerke J, et al. FDG uptake in breast cancer: correlation with biological and clinical prognostic parameters. Eur J Nucl Med Mol Imaging. 2002;29(10):1317–23.

96. Avril N, Menzel M, Dose J, Schelling M, Weber W, Janicke F, et al. Glucose metabolism of breast cancer assessed by 18F-FDG PET: histologic and immunohistochemical tissue analysis. J Nucl Med. 2001;42(1):9–16.

97. Shimoda W, Hayashi M, Murakami K, Oyama T, Sunagawa M. The relationship between FDG uptake in PET scans and biological behavior in breast cancer. Breast Cancer. 2007;14(3): 260–8.

98. Ikenaga N, Otomo N, Toyofuku A, Ueda Y, Toyoda K, Hayashi T, et al. Standardized uptake values for breast carcinomas assessed by fluorodeoxyglucose-positron emission tomography correlate with prognostic factors. Am Surg. 2007;73(11):1151–7.

99. Groheux D, Giacchetti S, Moretti JL, Porcher R, Espie M, Lehmann-Che J, et al. Correlation of high 18F-FDG uptake to clinical, pathological and biological prognostic factors in breast cancer. Eur J Nucl Med Mol Imaging. 2011;38(3):426–35.

100. Mavi A, Cermik TF, Urhan M, Puskulcu H, Basu S, Yu JQ, et al. The effects of estrogen, progesterone, and C-erbB-2 receptor states on 18F-FDG uptake of primary breast cancer lesions. J Nucl Med. 2007;48(8):1266–72.

101. Inoue T, Yutani K, Taguchi T, Tamaki Y, Shiba E, Noguchi S. Preoperative evaluation of prognosis in breast cancer patients by [(18)F]2-Deoxy-2-fluoro-D-glucose-positron emission tomography. J Cancer Res Clin Oncol. 2004;130(5):273–8.

102. Basu S, Chen W, Tchou J, Mavi A, Cermik T, Czerniecki B, et al. Comparison of triple-negative and estrogen receptor-positive/progesterone receptor-positive/HER2-negative breast carcinoma using quantitative fluorine-18 fluorodeoxyglucose/positron emission tomography imaging parameters: a potentially useful method for disease characterization. Cancer. 2008;112(5):995–1000.

103. Kumar R, Chauhan A, Zhuang H, Chandra P, Schnall M, Alavi A. Clinicopathologic factors associated with false negative FDG-PET in primary breast cancer. Breast Cancer Res Treat. 2006; 98(3):267–74.

104. van der Hoeven JJ, Krak NC, Hoekstra OS, Comans EF, Boom RP, van Geldere D, et al. 18F-2-fluoro-2-deoxy-d-glucose positron emission tomography in staging of locally advanced breast cancer. J Clin Oncol. 2004;22(7):1253–9.

105. Aukema TS, Rutgers EJ, Vogel WV, Teertstra HJ, Oldenburg HS, Vrancken Peeters MT, et al. The role of FDG PET/CT in patients with locoregional breast cancer recurrence: a comparison to conventional imaging techniques. Eur J Surg Oncol. 2010;36(4): 387–92.

106. Berg WA, Weinberg IN, Narayanan D, Lobrano ME, Ross E, Amodei L, et al. High-resolution fluorodeoxyglucose positron emission tomography with compression ("positron emission mammography") is highly accurate in depicting primary breast cancer. Breast J. 2006;12(4):309–23.

107. MacDonald L, Edwards J, Lewellen T, Haseley D, Rogers J, Kinahan P. Clinical imaging characteristics of the positron emission mammography camera: PEM Flex Solo II. J Nucl Med. 2009;50(10):1666–75.

108. Eo JS, Chun IK, Paeng JC, Kang KW, Lee SM, Han W, et al. Imaging sensitivity of dedicated positron emission mammography in relation to tumor size. Breast. 2012;21(1):66–71.

109. Levine EA, Freimanis RI, Perrier ND, Morton K, Lesko NM, Bergman S, et al. Positron emission mammography: initial clinical results. Ann Surg Oncol. 2003;10(1):86–91.

110. Rosen EL, Turkington TG, Soo MS, Baker JA, Coleman RE. Detection of primary breast carcinoma with a dedicated, large-field-of-view FDG PET mammography device: initial experience. Radiology. 2005;234(2):527–34.

111. Tafra L, Cheng Z, Uddo J, Lobrano MB, Stein W, Berg WA, et al. Pilot clinical trial of 18F-fluorodeoxyglucose positron-emission mammography in the surgical management of breast cancer. Am J Surg. 2005;190(4):628–32.

112. Berg WA, Madsen KS, Schilling K, Tartar M, Pisano ED, Larsen LH, et al. Breast cancer: comparative effectiveness of positron emission mammography and MR imaging in presurgical planning for the ipsilateral breast. Radiology. 2011;258(1):59–72.

113. Berg WA, Madsen KS, Schilling K, Tartar M, Pisano ED, Larsen LH, et al. Comparative effectiveness of positron emission mammography and MRI in the contralateral breast of women with newly diagnosed breast cancer. AJR Am J Roentgenol. 2012;198(1):219–32.

114. Cutler M. Transillumination of the breast. Ann Surg. 1931;93(1): 223–34.

115. Sickles EA. Breast cancer detection with transillumination and mammography. AJR Am J Roentgenol. 1984;142(4):841–4.

116. Leff DR, Warren OJ, Enfield LC, Gibson A, Athanasiou T, Patten DK, et al. Diffuse optical imaging of the healthy and diseased breast: a systematic review. Breast Cancer Res Treat. 2008;108(1):9–22.

117. Soliman H, Gunasekara A, Rycroft M, Zubovits J, Dent R, Spayne J, et al. Functional imaging using diffuse optical spectroscopy of neoadjuvant chemotherapy response in women with locally advanced breast cancer. Clin Cancer Res. 2010;16(9):2605–14.

118. Poellinger A, Persigehl T, Mahler M, Bahner M, Ponder SL, Diekmann F, et al. Near-infrared imaging of the breast using omocianine as a fluorescent dye: results of a placebo-controlled, clinical, multicenter trial. Invest Radiol. 2011;46(11):697–704.

119. van de Ven S, Wiethoff A, Nielsen T, Brendel B, van der Voort M, Nachabe R, et al. A novel fluorescent imaging agent for diffuse optical tomography of the breast: first clinical experience in patients. Mol Imaging Biol. 2010;12(3):343–8.

120. Jose I, Deodhar KD, Desai UB, Bhattacharjee S. Early detection of breast cancer: synthesis and characterization of novel target specific NIR-fluorescent estrogen conjugate for molecular optical imaging. J Fluoresc. 2011;21(3):1171–7.

121. van de Ven SM, Elias SG, Chan CT, Miao Z, Cheng Z, De A, et al. Optical imaging with her2-targeted affibody molecules can monitor hsp90 treatment response in a breast cancer xenograft mouse model. Clin Cancer Res. 2012;18(4):1073–81.

122. Shalviri A. Evaluation of new bi-functional terpolymeric nanoparticles for simultaneous in vivo optical imaging and chemotherapy of breast cancer. Drug Deliv Transl Res. 2012;2(6):437–53.